Sulfide-silicate textures in magmatic Ni-Cu-PGE sulfide ore deposits: massive, semi-massive and sulfide-matrix breccia ores.

Stephen J. Barnes1*, Sebastian Staude[2], Margaux Le Vaillant[1], Rubén Piña[3], Peter C. Lightfoot[4]

[1]CSIRO Mineral Resources, Perth, Australia. [2]University of Tuebingen, Germany. [3]Facultad de Ciencias Geológicas, Universidad Complutense de Madrid. [4]Lighfoot Geoscience Inc., Sudbury, Canada.

*steve.barnes@csiro.au

Highlights

- New nomenclature for Ni-Cu sulfide ores based on texture
- Review of observations on sulfide-matrix breccia ores
- So-called "remobilised" ores may be formed at magmatic melt-infiltration fronts

Abstract

Much of the value of magmatic Ni-Cu-PGE sulfide orebodies is contained within massive or semi-massive ores that show a wide variety of textural relationships to included or adjacent silicate rocks. We identify five mutually gradational textural types: (1) pure inclusion-free massive sulfide ores; (2) sulfide matrix ore breccias, of sharp-wall, soft-wall or mixed character; (3) emulsion textured ores formed by frozen mixtures of molten silicate and sulfide, most commonly developed as melt films at thermal erosion contacts; (4) vein-hosted sulfides formed at late magmatic or high temperature post-emplacement deformation stage close to the brittle-ductile transition in the country rocks or host igneous bodies; and (5) tectonic "durchbewegung" breccias, formed by mechanical inter-shearing of silicate inclusions and weak, ductile solid sulfides. Some deposits, the Moran Shoot at Kambalda being the type example, record the invasion of country rock footwall by downward- or sideways-percolating superheated molten sulfide liquid generating vertical sequences of pure massive sulfide, emulsion textured ores and finely-spaced invasive sulfide veins; these are referred to as sulfide melting-infiltration fronts and may provide a clue to the mechanism of formation of sulfide-rich magmatic ores as whole. Sulfide matrix ore breccias are particularly well developed in the Voisey's Bay and Aguablanca deposits, where they developed by flooding of percolating sulfide melt through the matrix of original silicate-matrix intrusion breccias. The lithology of the silicate or carbonate rock inclusions determines the nature of the inclusion-matrix relationships. Non-refractory inclusions typically disaggregate along original grain boundaries to leave coherent inclusions surrounded by clouds of inclusion-derived or matrix-derived crystals, with the low-melting silicate component preferentially displaced by sulfide liquid, whereas refractory inclusions retain sharp boundaries. Zonation of inclusions and overgrowths preserves reaction between inclusion and silicate matrix that pre-dates invasion of the intrusion breccia by sulfide liquid. The process of percolation of dense, low-viscosity sulfide liquid into pore space and fractures within partially molten (or melting) silicate rock is a unifying theme that links sulfide matrix ore breccias and emulsion textured ores with distinctive textures in less sulfide rich rocks such as net-texture (matrix ore texture), leopard texture (poikilitic net texture) and interspinifex ore. Vein-hosted massive sulfides may be emplaced under magmatic conditions where the excess pressure of the sulfide liquid column drives or enhances fracturing of the country rock and injection of sulfide into the cracks. Such veins are commonly referred to as "remobilised", a term which may obscure process understanding and should be reserved for cases where tectonic solid-state mobilisation of sulfide can be demonstrated on textural and structural grounds. The tendency of sulfide liquids to invade country rocks and potentially to drive the propagation of their own magmatic containers may be a critical feedback loop in the development of magmatic sulfide mineral systems.

1. Introduction

Magmatic sulfide ore deposits are some of the world's most valuable metal accumulations, currently accounting for ~56% of the world's nickel production (Mudd and Jowitt, 2014, Peck and Huminicki, 2016). They form by the accumulation of immiscible sulfide liquid that scavenged chalcophile elements from a coexisting silicate magma in various settings and became physically concentrated within magma reservoirs or flow pathways (Naldrett, 1997, Barnes *et al.*, 2016b). Information about the processes of accumulation and subsequent migration of the sulfide liquid can be derived from detailed study of textures of sulfide-silicate intergrowths (Godel *et al.*, 2013, Barnes *et al.*, 2017c, Barnes *et al.*, 2017d).

Magmatic sulfide ores fall into two major categories depending on the proportion of sulfide minerals in the ore (Barnes *et al.*, 2017a). The first category includes stratiform accumulations of disseminated sulfide in silicate or silicate - oxide cumulates within layered mafic-ultramafic intrusions, including PGE enriched "Reefs" (Mungall and Naldrett 2008; Naldrett 2011). The second, the subject of this contribution, comprises sulfide rich deposits where a high proportion of the value of the ore is in rocks containing 20% or more sulfide. This category includes deposits in small mafic or mafic-ultramafic intrusions, usually identifiable as magma conduits, examples of which include the deposits of the Noril'sk-Talnakh camp and Voisey's Bay (Barnes et al. 2016a; Lightfoot and Evans-Lamswood 2015); sulfide rich (Type 1) ores in komatiite lava flows (Lesher 1989; Lesher and Keays 2002; Barnes 2006) such as those at Kambalda or in shallow subvolcanic ferropicrite intrusions as at Pechenga (Hanski 1992; Keays 1995; Hanski et al. 2001); and the Sudbury ores associated with an impact melt sheet (Lightfoot, 2016).

Typically, the assemblage of ore types in sulfide-rich deposits contains a large component of massive or semi-massive ores, characterised by the presence of modal sulfide proportions between about 50 and 100% on sample length scales of tens of centimetres to tens of metres (Naldrett, 2004). These ores consist predominantly of the characteristic magmatic sulfide mineral assemblage: pyrrhotite, chalcopyrite, pentlandite with or without minor pyrite, reflecting low temperature unmixing of magmatic sulfide liquids with a restricted range of metal:S ratios dictated by magmatic silicate-sulfide liquid equilibrium (Naldrett, 1969, Naldrett, 2004). In most if not all these deposits, at least some proportion of the ore consists of semi-massive sulfide where silicate inclusions are present in a continuous matrix of solidified sulfide magma. Despite their ubiquity, such semi-massive ores have received relatively little systematic study. This contribution follows on from a companion paper on textures in disseminated and net textured ores (Barnes *et al.*, 2017d) to present a systematic catalogue, classification and interpretation of the variety of silicate-sulfide intergrowths encountered in the spectrum of magmatic sulfide ores. We aim to bring some systematic order to the nomenclature of these ore types, and to use our observations to constrain hypotheses for their origins.

2. Methods and Samples

The observations reported here are based on several decades of research on magmatic Ni-Cu-PGE ores, with a focus over the last few years of documenting and imaging the diversity of textures observed in nature at the scale of drill core and underground mine openings. Observations are complemented with optical microscopy and in many cases by micro-beam XRF element mapping (XFM) on polished thin sections and cut surfaces of drill core or hand samples, a technique that can reveal much relevant detail and complexity easily overlooked by the naked eye. In some cases we have also investigated textures in three dimensions using x-ray tomography at hundred-micron resolution in a medical CT scanner. The XFM and medical CT imaging methodology have been described in detail by Barnes et al (2017b,c). Samples have been collected from a number of deposits including all the settings outlined above: intrusive and extrusive komatiite-hosted; small conduit style intrusions, and from Sudbury. Brief descriptions and reference sources are listed in Table 1, and covered in more detail in the text for some of the critical localities.

False colour XFM element maps are derived by scaling the X-ray count rates for each pixel to a user-defined minimum and maximum value for each selected element over the entire image, and assigning each of three selected elements to the red, green or blue channels of a 24-bit (8 bits, or 256 shades, per channel) RGB colour bitmap. This gives rise to distinctive colours for particular phases. In some cases, these maps can be used effectively to show distribution of phases, but in most cases it is necessary to use a larger number of elements to identify all the important phases in a sample. In these cases, phase maps were obtained in most cases by generating a number of different three-element maps, then using the colour selection wand tool in Adobe Photoshop™ image processing software to select and create colour masks attributable to particular phases.

Table 1, localities

3. Previous work

Massive and semi-massive ores have been mentioned or described in passing in a large number of publications on magmatic ores, but relatively few publications have focused on them specifically from the point of view of textures and emplacement mechanisms. Of these, most have been concerned with komatiite-hosted ores which, as we will see, have some distinctive characteristics of their own. These studies (Frost and Groves, 1989, Dowling *et al.*, 2004, Staude *et al.*, 2016, Barnes *et al.*, 2017c, Staude *et al.*, 2017a) focus largely on dynamic processes at silicate-sulfide melt interfaces, and provide a key set of observations defining end-members of the natural range of ore types. A number of studies at Sudbury, comprehensively reviewed by Lightfoot (2016), deal with the special case of massive sulfide occupying sharp-walled veins in country rocks, representing the case of physical migration of dense sulfide liquid into adjacent open fractures. Broadly similar features at Voisey's Bay are described and interpreted by Saumur and Cruden (2017).

Sulfide-matrix breccia ores, defined by the presence of coherent silicate rock fragments in a continuous matrix of magmatic sulfide (Barnes et al., 2017c), have received little attention with the exception of those at Voisey's Bay (Evans-Lamswood *et al.*, 2000, Li and Naldrett, 2000, Mariga *et al.*, 2006b, a, Barnes *et al.*, 2017c) and Aguablanca (Tornos *et al.*, 2001, Ortega *et al.*, 2004, Piña *et al.*, 2006, Pina *et al.*, 2010, Barnes *et al.*, 2018). In both these cases, ore breccias consist of polymict assemblages of country rock xenoliths and endogenous autoliths. At Voisey's Bay, essential features of these breccias have been variously interpreted as products of upward-emplaced slurries of sulfide melt with entrained xenoliths (Evans-Lamswood *et al.*, 2000) or as the result of percolation of dense sulfide melt downward into the inter-inclusion porosity of pre-existing silicate intrusion breccia (Barnes et al., 2017b). The latter process has also been invoked for the sulfide-matrix breccias at Aguablanca (Barnes *et al.*, 2018), invoking a continuum with intercumulus sulfide melt percolation in the formation of net textured ores and spinifex ores (Barnes *et al.*, 2016a, Barnes *et al.*, 2017d). This percolation mechanism is a form of density-driven viscous fingering, governed by differential densities and surface wetting characteristics of two fluids of contrasting density, viscosity and wetting characteristics migrating through a porous medium (Chung and Mungall, 2009). The continuity of this process from small scales in cumulate rocks to larger scales in intrusion breccias is a key finding of this study.

4. Nomenclature

The nomenclature of sulfide rich ores is currently unsystematic, such that some initial definitions are necessary. We begin by defining a set of terms for the main textural types, then expand on this with reference to some specific type localities, then conclude by proposing a classification scheme. (This sequence has the disadvantage that in some cases observations at different scale from the same deposit are split between a number of different figures, but this is necessary to maintain the development of the argument).

The main challenge is to devise a set of terms and rock names that are essentially descriptive and depend as little as possible on prior assumptions about genetic processes. Particularly with breccia ores, there are no clearly defined criteria for distinguishing primary magmatic ores from tectonic ores formed by mechanical incorporation of silicate fragments into a sulfide matrix during solid state deformation, a point we discuss in Section 6 below. For clarity in what follows, we propose the following nomenclature based as far as possible on directly observable characteristics with minimal genetic overlay. These terms are intended to be used at hand sample scale, i.e. at a length scale of tens of centimetres that can usefully be applied during core logging and outcrop or underground mapping.

Massive ores consist of upward of 90% sulfide by volume, with variable but typically low proportions of oxides, and are commonly free of silicate inclusions altogether, particularly where massive sulfide pools are more than a few metres thick. Silicate inclusions where present are dispersed and isolated, i.e. not in direct contact as observed in 2D surfaces.

Semi-massive ores, called "inclusion massive ores" at Sudbury, form a continuum between massive ores and sulfide-matrix ore breccias with variable abundance of silicate inclusions down to about 20% by volume.

Sulfide matrix ore breccias comprise silicate mineral inclusions in a continuous matrix of sulfide, regardless of mode of origin, and form a continuum toward *vein array breccias* (Figure 1). Based on the nature of silicate-sulfide contacts, and the nature of the silicate inclusions, the category can be further subdivided. The term "breccia" is retained regardless of whether the inclusions are angular or rounded, although some varieties are not breccias at all in the usual sense of the term as applied to tectonic, sedimentary and hydrothermal breccias. (We use the non-genetic term "inclusions" rather than "clasts" for this reason).

Figure 1. Underground face photos showing sharp-wall inclusion breccias and sulfide breccia veins.

One of the major types of variability within sulfide matrix ore breccias lies in the nature of the inclusions, and particularly their margins. Inclusions can be loosely categorised into sharp-walled and soft-walled types, illustrated at outcrop scale in Figs. 1 and 2. In some cases these can be found within the same rock, where the nature of inclusion contacts varies depending upon lithology, but it is useful to subdivide breccia types according to the dominant type of inclusion. Sharp-walled inclusions show little or no sign of disaggregation or strain partitioning at their margins (Figure 1), may be rounded or angular and in some cases show jig-saw fit features. Soft-wall inclusions are marked by a prevalence of disaggregated margins breaking down into individual crystals within the surrounding sulfide matrix. The breakdown of inclusions can be accompanied by melting, forming a continuum to emulsion-textured ores. Both sharp- and soft-wall inclusions show wide size distributions ranging from m to mm scale, usually with no evidence of size sorting.

A significant variant of sulfide matrix breccias with soft-wall inclusions is characterised by highly irregular and often self-similar sinuous contacts between silicate and sulfide melts, with evidence for the silicate inclusions having been molten at the time of incorporation (Figure 2, Figure 3). The upper range of inclusion sizes is typically much less than in sharp-walled inclusions. Such textures in most cases are likely to be the result of solidification of silicate-sulfide immiscible melt emulsions, and were taken as evidence of such in one of the landmark papers that established the magmatic origin of the Sudbury sulfide ores (Figure 3) (Hawley, 1962). They typically occur at the interface between massive ores and country rocks, in some cases as a laterally persistent mixed-melt film at the contact. For this type, since they are the furthest from being actual breccias in the conventional sense of the term and since their interpretation is relatively non-contentious, we make an exception to the rule of using non-genetic terminology and refer to them from here on as *emulsion-textured ores*.

Figure 2. Underground face photos…

Figure 3 Hawley Sudbury emulsion sample and other emulsion textures…

Vein-array breccias (Figure 1C,D,F) are the result of isolation of wall rock fragments between multiple crosscutting or anastomosing sulfide-filled veins, which are usually sharp-walled but can also be soft-walled, and which themselves commonly contain “floating” wall rock fragments. They are usually but not exclusively monomict, with inclusions of widely ranging sizes being derived from the immediate wall rock. There is commonly a continuum between this type and more conventional breccias as the abundance of sulfide and thickness of the veins increases (e.g. compare Figure 1C,D,E,F), and with durchbewegung breccias where the veins localize shearing. Much of the ambiguity in interpretation between magmatic sulfide migration and solid-state tectonic remobilisation concerns this category.

Durchbewegung breccias form predominantly in the solid state by deformation. They are defined by the development of concordant foliations in both silicate and sulfide components, typically sharp-walled inclusions with thin shear bands developed along the inclusion margins, folding of inclusions, development of pentlandite bands reflecting exsolution along original aligned pyrrhotite basal partings, and local or pervasive development of mylonitic fabrics and strong lineations, discussed further below. They are typically localized within recognizable planar shear zones, often at country rock contacts.

5. Case studies: modes of occurrence of massive and semi-massive ores

In this section, we describe a number of case studies that exemplify occurrences of the different textural types outlined above and show how they relate spatially to one another. The chosen examples are derived from a number of settings: contact ores in komatiites and mafic-ultramafic sills; sulfide accumulations at propagating tips of bladed dykes (Barnes and Mungall, 2018); sulfide-matrix breccias in funnel necks and dyke bridges (bridge-like connections between offset dyke segments); and strongly deformed durchbewegung ores in highly tectonised host and country rocks. A number of common genetic processes become clear from these diverse examples.

5.1. Melt-Infiltration Contact Ores and Emulsion Textures

The most familiar and widely recognised mode of occurrence of massive ores is at basal contacts between the host intrusion, or host flows in the case of komatiite hosted ores, and their country rocks. Sulfide-matrix breccia ores at such contacts commonly include melt-infiltration fronts and emulsion-type ores formed where the country rock was melting while the sulfide liquid was being emplaced.

5.1.1. Moran and McLeay, Kambalda

The Moran deposit, on the east flank of the Kambalda Dome in the Archean Kalgoorlie Terrane in Western Australia, is an exceptionally well preserved example of massive sulfide and sulfide matrix breccias in a contact position in a komatiite flow (Staude *et al.*, 2016, Staude *et al.*, 2017a). Similar textures are also seen in the McLeay shoot, also forming part of the Long-Victor underground operation. Moran and McLeay both have the typical characteristics of Kambalda style contact ores (Type 1 ores in the terminology of Lesher and

Keays (2002)), comprising elongate "shoots" of massive sulfide within topographic embayments in the footwall basalt surface at the base of a thick sequence of channelised komatiite flows. The base of the Moran massive sulfide is an example of a sulfide infiltration-melting zone, with a characteristic progression of textures shown in outcrop-scale in Figure 2A and in detail in Figure 4. Inclusion-free massive sulfide ore overlies a zone of emulsion-textured ores developed as a film up to 10 cm wide along the contact with the football basalt (Figure 4A). This film acts as a Rayleigh-Taylor instability (a layer of less dense fluid below denser fluid) and locally develops into dome-shaped plumes of basaltic melt (Figure 4B,C, E), surrounded by haloes of skeletal ferrian chromite within the adjacent sulfide (Figure 4F) (Staude *et al.*, 2016, Staude *et al.*, 2017a). Beneath this zone, there is either a transition through a zone of finely disseminated sulfide in basalt into solid sulfide-free basalt footwall, or in places sulfide infiltrates into the footwall as a series of downward-propagating anastomosing veinlets. Narrow melt films of basalt are developed at the vein margins in the upper few cm, picked out in the XFM images (Figure 4) by presence of fine grained chromite that develops by reaction between the silicate and sulfide liquids. These films disappear downwards through a transition into a zone of vein array breccia that locally penetrates usually a few cm but locally as much as a metre into the footwall (Figure 2A). Thickest development is in places where the sulfide melt is invading a pre-existing inter-pillow breccia.

Figure 4 Moran emulsion/infiltration details.

One remarkably preserved underground exposure at Moran contains an example of emulsion-textured ore formed by upward ponding of "floating" silicate melt at the top of a massive sulfide pool, in a "pinchout" setting where sulfide liquid has migrated laterally to have country rock as both floor and roof (Figure 5). An array of textures is preserved including plumose bands of chromite developed at interfaces between nearly pure sulfide and silicate-rich emulsion (Figure 5A), and cm-scale banding between sulfide-rich and sulfide-poor layers containing amphibole replacing original skeletal clinopyroxene and finely skeletal chromite developed beneath a layer of vesicular basaltic "scum" (Figure 5B, C, D). The detailed interpretation of these textures is discussed by Staude et al. (2016).

Figure 5 Moran roof-ponding emulsions

5.1.2. Silver Swan

A similar example of a sulfide infiltration-melting zone beneath an originally horizontal komatiitic contact orebody is in the Silver Swan deposit at Black Swan, 150 km north of

Kambalda (Dowling *et al.*, 2004, Barnes *et al.*, 2017b). Here the footwall is dacite rather than basalt, giving rise to a zone of emulsion textured ores up to 5m wide along the basal contact, above a zone of sulfide vein injection into the dacite footwall. Emulsion textured ores consist of sinuous, disaggregating inclusions of dacite preserving their original textures in their cores but showing evidence of melting followed by quench crystallisation at their margins.

Silver Swan emulsion textured ores display an unusual texture (Figure 6A), also seen at Moran (Figure 4D. Fig. 6B) where emulsions are generated by melting of sediment rather than basalt. Where the dacite "blobs" have broken up into particularly fine aggregates, they form a kind of inverted net textured ore where silicate melt (now a granophyric intergrowth of quartz and feldspar) occupies interstices between idiomorphic pyrrhotite grains, originally crystallised as MSS (Figure 6). As discussed by Staude et al (2017) at Moran (Figure 6B) and Barnes et al. (2016c), this is a consequence of the relative melting ranges of the silicate and sulfide melts: Cu-poor sulfide melt crystallises before the dacitic silicate melt does. Similar textures have been observed in a number of different deposits, including non-komatiitic settings such as Nebo-Babel where ores are associated with granophyric partial melts of the felsic country rocks (Figure 6C).

Figure 6 Inverted net textures – SS, Moran, Nebo-Babel

5.1.3. Eagle, Michigan

The Eagle deposit in the Mid-Continent Rift of the USA is one of a number of small mineralized conduit-style intrusions associated with the 1100 Ma large igneous province that also incorporates the Duluth Complex and the Keeweenaw flood basalts (Keays and Lightfoot, 2015). Massive and semi-massive ores occupy the keel of a narrow boat-shaped to funnel-shaped intrusion (Figure 7A) thought to represent a zone of widening within a predominantly vertical dyke or narrow funnel (Ripley and Li, 2011, Ding *et al.*, 2012a, Ding *et al.*, 2012b). The deposit is almost completely undeformed and shows only low grade metamorphism.

Figure 7 Eagle, VB and Aguablanca – schematic sections

Underground exposures in the Eagle Mine show some remarkably well preserved primary magmatic contacts where massive sulfide is in contact with organic-rich and locally sulfidic black shales. Sulfide melt injects as sills from a few cm to several m thick along bedding planes of the shale, causing planar sheets of shale to peel back and partially float into the sulfide pool (Figure 2C, Figure 8A,B,C). A silicate melt film is developed over a thickness of about 20cm, most clearly at horizontal surfaces, where it forms cm-dm scale plumes and “blobs” of molten silicate melt that partially detach from this surface and float into the sulfide, forming emulsion-textured ores (Figure 8D,E). The relationship is very similar to that reported from the Kharealakh Intrusion, Siberia, by Sluzhenikin et al. (2014), whose photograph is reproduced as Figure 2B.

A notable feature of these contacts is that the massive sulfide is almost completely devoid of silicate melt inclusions above this film-plume zone, a feature also seen at Silver Swan, Voisey’s Bay and Kharealakh where substantial thicknesses (10m or more) of very clean massive sulfides overlie melt emulsion contacts. The implication is that when the silicate melt blobs detach from the floor, they float rapidly away into the sulfide owing to their much lower density, and in this case are probably swept away by lateral flow of sulfide. Only in rare cases such as that described above at Moran and also by Dowling et al. (2004) at Silver Swan does silicate melt formed in this way become preserved at the top of the sulfide pool.

Figure 8. Emulsion textures developed at a sulfide melting-infiltration front at the basal and lateral contacts of massive sulfide ore at Eagle.

5.2. Sulfide Matrix Breccia ores

5.2.1. Sulfide matrix breccias – Sudbury

One of the principal ore types in the contact and offset type deposits of the Sudbury Igneous Complex comprises a matrix of sulfide with floating or imbricated inclusions of mafic to ultramafic rocks (Figure 9). The inclusions are locally infiltrated and replaced by the matrix sulfide, and the margins of the inclusions commonly have elevated chalcopyrite concentrations (e.g. Fig. 9C, right) representing residual sulfide liquid after MSS crystallisation. This ore type tends to be restricted to the Sublayer embayments and the Offset dykes. Massive sulfides at Sudbury are more commonly contained in the country rocks adjacent to the contact deposits, and they are marked by very rare inclusions (e.g. the footwall deposits at Victor, Nickel Rim, and Levack-Coleman in the North Range and the Creighton Depth deposit in the South Range; Lightfoot, 2016). In cases where sulfides have been transported during deformation, the textures more commonly resemble sulfide matrix breccias with abundant fragments from the local country rocks, sheared margins, and unusual sulfarsenide mineral associations. These sulfide ores are transitional in nature from the sulfide matrix breccias in the Sublayer through to durchbewegung breccias in shear zones that cross-cut these contact ores. Examples include the shear-zones in the Garson (Fig. 9B), Falconbridge, and Crean Hill Deposits (Lightfoot, 2016).

The difference between the tectonically modified style of mineralization and the primary magmatic association found in the Sublayer is evident from the geological setting (Sublayer versus shear zone), fabric and deformation textures in the sulfide, and the presence of very distinctive durchbewegung textures.

Figure 9. Sudbury ore breccias…

5.2.2. Sulfide matrix breccias – Voisey's Bay

The Voisey's Bay ores are hosted within a complex mafic sill-dyke network forming part of the Nain Plutonic Province in Labrador (Naldrett *et al.*, 1996, Ryan, 2000) (Figure 7B). Ores range from exceptionally thick and pure massive sulfide bodies such as the Ovoid to breccia-dominated ores developed within thickened zones of olivine gabbro and troctolite dykes and intersections between dykes and (originally) horizontal sills (Evans-Lamswood *et al.*, 2000, Lightfoot *et al.*, 2012). Ores are strongly localised by intersections of pre-existing planar fault sets and foliations (Saumur *et al.*, 2015, Saumur and Cruden, 2016).

Sulfide matrix breccias at Voisey's Bay are a widespread component of the ore system, occurring in close association with, and commonly directly beneath, massive ores (Figure 7B). A sequence of several m thickness of breccias lines the base of the Ovoid orebody, and fills the central portion of the main ore-bearing dyke in the Reid Brook Zone (Lightfoot *et al.*, 2012), interpreted as a bridge between two offset segments of the dyke (Saumur and Cruden, 2015).

Sulfide matrix breccias are developed within a range of rock types from polymict intrusion breccias, with rock fragments in sulfide-poor troctolite or olivine gabbro matrices, to heterogeneous "vari-textured" gabbros with rapid short range variations in grain size and content of hydrous phases (Lightfoot *et al.*, 2012). Rock fragment populations in the breccias include endogenous gabbros (cumulate and non-cumulate) and cumulate peridotites along with extensively depleted plagioclase-hercynite gneisses (Evans-Lamswood *et al.*, 2000, Li and Naldrett, 2000) interpreted as restites from extensive partial melting of country rock quartzo-feldspathic paragneisses (Mariga *et al.*, 2006b).

Both sulfide-poor and sulfide-rich breccias (Figure 10) comprise heterolithic assemblages of inclusions within a matrix of olivine gabbro (Barnes *et al.*, 2017c). This matrix is characterised by an interconnected 3D framework of plagioclase crystals, highly variable in grain size at mm to cm scale, with interstitial olivine and poikilitic clinopyroxene, and is texturally indistinguishable from inclusion-free olivine gabbro (Figure 10B-E). Sulfide forms interconnected networks at cm to dm scale and possibly larger, even where the sulfide content of the rock is as low as 10% by volume. Much of the plagioclase developed by outgrowth from the margins of paragneiss xenoliths when the porosity was occupied by silicate melt. These gneiss inclusions are actually sharp-walled, although this is obscured by this subsequent overgrowth of plagioclase.

The observed range of textures is explained by a model of percolation of molten sulfide through variably crystalline inter-inclusion matrix, displacing the silicate melt to leave the refractory plagioclase-olivine or in some cases plagioclase-only component, now entirely within a sulfide matrix. The process is analogous to that believed to have formed interspinifex ore in komatiite-hosted deposits (Groves *et al.*, 1986, Barnes *et al.*, 2016a), Biotite rims on plagioclase enclosed in sulfide are interpreted as the result of reaction between plagioclase, olivine and a hydrous component derived from the sulfide melt itself, with a possible component of migrating residual silicate melt wicking along sulfide-silicate contacts.

Figure 10 VB breccias – essential features

5.2.3. Sulfide matrix breccias – Aguablanca, Spain

The Aguablanca Ni-Cu deposit in south-western Spain is hosted by the Aguablanca stock, a funnel-shaped mafic body composed of gabbronorite and minor quartz-diorite, gabbro, and norite (Piña *et al.*, 2006). The main body of the intrusion consists of gabbronorites with minor ultramafic cumulates, and marginal zones of taxitic gabbro containing similar assemblages of silicate inclusions as the sulfide ore breccias (Figure 11A). Sulfides are concentrated in a gabbronorite matrix along a subvertical (dip of 70º–80º N), funnel-like magmatic breccia developed within the core of the intrusion (Figure 7C) that contains barren or slightly mineralized ultramafic-mafic cumulate fragments. Modal compositions of the silicate fragments in the SMOBs reflect a wide variety of rock types, including peridotite (hornblende-rich werhlite, dunite, and hornblende-rich harzburgite), pyroxenite (ortho- and clinopyroxenite), gabbro (gabbro, gabbronorite, and hornblende gabbro), and anorthosite along with a diverse assemblage of metasediments and skarn rocks derived from the immediate country rocks. The sulfide-matrix breccias are mantled by a concentric zone of disseminated sulfides within gabbronorites, showing strong petrographic similarities to the silicate component of the matrix of the breccias and the main unmineralized gabbronorite (Figure 11). As at Voisey's Bay, a continuum exists between breccias with predominantly sulfide matrices to breccias with similar inclusion assemblages in a matrix of pyroxenitic melagabbro or taxitic gabbro (Figure 11A) with sparse disseminated sulfide.

Breccia textures have been investigated at mm to cm scale (Barnes *et al.*, 2018), revealing a number of distinctive common features: disaggregation of inclusions into adjacent sulfide along original silicate grain boundaries (Figure 11BC,E); complex reverse and oscillatory zoning in Cr content of clinopyroxene grains both as isolated crystals within sulfide and embedded in inclusions (Figure 11E,F); relatively minor reaction rims with enclosing silicates on some country rock inclusions; and preferential disposition of pyroxene crystals within pyrrhotite-pentlandite aggregates (original MSS) relative to inclusion-poor chalcopyrite (Figure 11C, arrowed). Inclusion-sulfide contacts take a number of different forms, in some cases within the same sample: cuspate textures representing melt emulsion mixtures (Figure 3F); grain-boundary disaggregation giving soft-walled inclusions; and sharp boundaries with sub-mm reaction rims on refractory calc-silicate inclusions. Figure 11D shows a relatively sulfide-poor sample where calc silicate inclusions are embedded within pyroxenitic gabbro that has been infiltrated by sulfide; the relationship of inclusions, inter-inclusion silicate and sulfide is very similar to that observed in the Voisey's Bay breccias where the inclusions are refractory hercynite spinel-bearing paragneisses (Figure 10).

Figure 11. Characteristic features of silicate- and sulfide-matrix ore breccias from Aguablanca.

The observed range of textures is explained by Barnes et al. (2018) by a model of downward percolation of molten sulfide through a pre-existing silicate-matrix intrusion breccia, preferentially displacing a cotectic or eutectic plagioclase-pyroxene melt. The process is analogous to that responsible for the superficially similar sulfide matrix ore breccias at Voisey's Bay described above, the differences being due to the composition of the inclusions and the original silicate magma (olivine-plagioclase saturated at Voisey' Bay, pyroxene-saturated at Aguablanca). The original intrusion breccia may itself may have been emplaced from above into the neck of the Aguablanca stock in the waning stages of magma flow through an extensive sill-dyke network. Sulfide percolation occurred simultaneously with sulfide crystallisation, forming large grains of MSS that trapped silicate grains and prevented them from floating up through sulfide liquid; these become preserved as frameworks of (often zoned) pyroxene crystals within pyrrhotite/pentlandite aggregates (Figure 11C). Timescales for sulfide percolation on a scale of metres were estimated by Barnes et al. (2017c) at days to months, compared with timescales for solidification in small intrusions of hundreds to thousands of years (Barnes and Robertson, 2018), giving plenty of time for the process to take place.

The sulfide infiltration model proposed for both Aguablanca and Voisey's Bay offers an alternative to the current model for upward emplacement of a slurry of silicate melt, sulfide melt and breccia fragments as a late stage injection into the dyke-sill complex. The preserved range of textures is interpreted as being due to gravity-driven percolation of sulfide liquid through a pre-existing partially molten intrusion breccia, which serves as a physical trap site, for the migrating sulfide liquid.

5.2.4. Skarn breccia – Oktyabrysky

The super-giant Ni-Cu-PGE orebodies of the Noril'sk-Talnakh camp (Likhachev, 1994, Lightfoot and Zotov, 2014) contain a very wide variety of sulfide textures, including globular ores with associated vapour bubbles (Le Vaillant *et al.*, 2017). Some of the most remarkable ores are sulfide-rich skarns. The example illustrated here (Figure 12) is a sample of a sulfide-matrix ore breccia with calc-silicate inclusions developed in an "exoskarn" on the lateral flanks of the Oktyabrysky massive sulfide orebody at the base of the Kharealakh intrusion (Sluzhenikin *et al.*, 2014). Original carbonate (presumably calcite) inclusions have been extensively replaced by wollastonite, with relic inclusions of intergrown calcite and anhydrite. The inclusions all show continuous haloes of magnetite; this is developed within the sulfide, at a regular and constant distance of 1-2 mm away from the margin of the calc-silicate inclusion (Figure 12B, C, D). In some cases, the inclusions themselves appear to have been extensively replaced by sulfide. Other inclusions show clear concentric zoning (Figure 12A). The sulfide matrix itself shows clear magmatic textures, showing the exact same relationship of pyrrhotite and exsolved pentlandite (Figure 12E,F) as observed in all other clearly magmatic Noril'sk-Talnakh ores.

The magmatic textures and mineralogy of the sulfide matrix indicate that these textures are not, as they first appear, the result of dissolution-precipitation replacement of carbonate by sulfide. A possible explanation is that skarns were developed over a prolonged period of interaction between country rocks and volatile-rich mafic magma flowing through the chonolith, before the final emplacement of sulfide, within carbonate rocks that were highly reactive but also highly refractory, and thus unable to melt and disaggregate in the way clastic sedimentary casts evidently did in the Savannah and Aguablanca examples. By analogy with Aguablanca and Voisey's Bay, we suggest that the magnetite haloes may be relics of an earlier stage in the history of this rock as a silicate matrix intrusion breccia, forming by progressive dissolution of carbonate inclusions into silicate melt leaving magnetite at the original inclusion boundary. This magnetite may also have crystallised from the sulfide melt analogously to the growth of chromite in the Moran examples. In this hypothesis, the silicate matrix was then flushed out by invading sulfide liquid. However, much remains to be learned about these intriguing rocks.

Figure 12 Oktyabrysky skarn breccia sample

5.2.5. Sulfide matrix breccias - Savannah

The Savannah (formerly known as Sally Malay) Ni-Cu ores in the Mesoproterozoic Halls Creek Orogen of Western Australia are dominated by sulfide-matrix ore breccias, showing evidence of primary magmatic origin with a variable tectonic overprint (Hicks *et al.*, 2017). They show some characteristic features in common with the aforementioned deposits, but also make for an informative case study of the problems in discriminating between magmatic and tectonic origins.

Two distinct but texturally very similar deposits are found within two adjacent mafic-ultramafic intrusions (Hicks *et al.*, 2017), emplaced at mid-crustal depths within granulite facies paragneisses of the Central Zone of the Halls Creek Orogen, which was generated by collision of the North Australian and Kimberley Cratons at ~1840-1830 Ma (Hoatson and Blake, 2000, Kohanpour *et al.*, 2017). The original Sally Malay deposit (now Savannah) is a 5.5 mt deposit grading 1.75% Ni and 0.66% Cu, consisting almost entirely of sulfide matrix breccia ores occupying the basal contact of a bladed dyke (Barnes and Mungall, 2018), now rotated through 90^{o} about an axis normal to the wall of the dyke, such that the orebody and the original cumulus layering in the intrusion now dip almost vertically. A schematic reconstruction of the original geometry is shown in Figure 7D.

Savannah ore breccias are typically polymict. Inclusion assemblages include fine-medium grained paragneiss of widely variable composition including abundant garnet rich metapelite lithologies as well as foliated garnet-poor meta-psammite lithologies (Figure 13A,B); unfoliated norites interpreted as being derived from the chilled margin of the host intrusion, and relatively rare inclusions of tonalite (Figure 13C,D). Commonly these inclusions show the same type of grain-boundary disaggregation at their margins as those at Aguablanca, giving rise to predominantly soft-wall inclusion breccias, but differing in that the disaggregated-crystal population within the sulfide matrix is commonly distinct from mineral assemblages in the neighboring inclusion (e.g. Figure 13E,F). Inclusions with partial or complete rims of garnet are common among the paragneiss assemblage, but the reverse is also present: garnet-rich inclusions with feldspathic, garnet poor rims (compare Figure 13B and F). Disaggregation of garnet-rich inclusions locally gives rise to “floating” garnet grains entirely within sulfide (Figure 13F).

A likely explanation is that, like the Aguablanca breccias, these rocks were formed by sulfide flooding of original complex silicate matrix breccias with a hybrid norite-tonalite groundmass, now almost completely displaced but present as local relics and around rims of inclusions. However, the more complex relationship between inclusion and single crystal inclusions, the presence of folded silicate inclusions (Figure 13E,F,G-I) and the local strong development of foliation in both inclusion and sulfide matrix, indicates a varying degree of deformation, specifically shearing.

The Savannah ores are well exposed in underground workings (Figure 1A,B,D), and show a number of characteristics reflecting a combination of undoubtedly tectonic and ambiguous but most probably magmatic features. Irregular sharp-walled veins are commonly developed within the originally overlying peridotite cumulates in the intrusion (Figure 1D) and in the paragneiss country rocks. In some case these veins clearly cross-cut breccia inclusions (Figure 14) and must represent either very late magmatic or solid-state postmagmatic remobilisation of sulfides into brittle fractures. In many cases these veins (as in Figure 14) show local enrichment in chalcopyrite in their tips, implying that they formed at a late magmatic stage when the Cu-rich, low-melting residual liquid from fractional crystallisation of sulfide was still mobile, implying temperatures around $800^{o}C$ (Craig and Kullerud, 1969). Inclusion-rich massive sulfides have clearly been mobilised in the solid state into fault zones in places, probably due to preferential fracturing along weak planar bodies of sulfide, and in these cases the breccias show undoubted typical durchbewegung textures, as discussed further in the next section.

Figure 13 Savannah breccias, core slabs – transition from definite durchbewegung to probable magmatic.

Figure 14 Savannah vein set

5.3. Tectonic (durchbewegung) breccias

Typical examples of durchbewegung sulfide breccias from two intensely deformed nickel sulfide deposits, Thompson and Spotted Quoll (Table 1) are illustrated in Figure 15. The Thompson example consists of quartz-rich metasediment inclusions in a matrix of sulfide, with a pronounced planar fabric defined both by the mineral banding in the silicate inclusion and by pentlandite exsolving along the preferred pyrrhotite orientation defining a parallel foliation. The pyrrhotite commonly shows evidence of kink banding and/or the development of a granular texture with triple junctions between pyrrhotite grains. The Spotted Quoll sample is a sulfide-rich mylonite, showing a similar strong alignment of pyrrhotite foliation and exsolved pentlandite, a strong planar alignment of silicate inclusions, and a pronounced L-tectonite lineation within the foliation. Silicate inclusions are strongly chloritized mafic country rock.

A characteristic of the Savannah breccias, illustrated in Figure 13, is the transition from weakly deformed or largely undeformed fabrics displaying similar features to the Aguablanca examples, to clearly tectonised durchbewegung breccias with strong fabrics defined by both silicates and sulfides (Figure 13 G,H,I). There is no way to know whether these breccias are purely tectonic in origin, originating by mechanical mixing of originally clean massive sulfide and tectonically entrained wall-rock clasts, or whether they start out as magmatic Aguablanca-style breccias that then become deformed as a result of preferential partitioning of strain into the weak sulfides during deformation. The absence of clean massive sulfides without inclusions, and the complete spectrum from undeformed to strongly deformed examples, some of which are clearly occupying late-stage shear zones cutting the orebody, tends to favour the view that these are tectonised magmatic breccias.

Figure 15 Durch and mylonite breccias

6. Genetic processes in semi-massive ores

6.1. Emulsion-textured ores and sulfide melt-infiltration fronts

Emulsion textured ores are the result of mingling of immiscible sulfide and silicate melts due to detachment and diapirism of buoyant silicate melt films at magmatic contacts, and disaggregation of silicate rock inclusions due to melt film generation at grain boundaries close to hot sulfide liquid (Figure 16). Such processes may develop at the basal or lateral contacts between sulfide liquid pools and underlying homogeneous country rocks, or during percolation of sulfide liquid through variably molten silicate matrix intrusion breccias as discussed in the following section. The key factor is that the process of interaction is frozen in place; at least one of the two liquids must freeze, or at least solidify to the extent of a rapid increase in viscosity, before the buoyant silicate melt blobs can detach and float out of the sulfide (the process that is effectively caught in the act in the Silver Swan and Moran examples).

Figure 16. Moran sulfide infiltration carton.

Ideally, and as observed at Moran (Figure 16), emulsion textured ores form the top of a melting-infiltration zone, the lower part of which comprises monomict sulfide-vein array breccias formed by intersecting and anastomosing sulfide veins penetrating into country rocks below. The process is driven by the hydrostatic head of the sulfide liquid column (Saumur and Cruden, 2017) causing sulfide liquid to be forced downward into microfractures once its column thickness exceeds a critical height. Excess pressure acts in all directions at the tip of propagating sulfide-filled cracks; hence veinlets can form and expand in any direction, with the dominant control being the local stress field and the existence of pre-existing fracture sets in the rock. The ultimate example of this process is in the Offset Dykes at Sudbury, where extensive fracture networks were generated by a bolide impact (although in these cases little or no melting of the wall rock occurs during sulfide emplacement). The same process was initiated at Kambalda by pre-existing jointing in submarine basalts, fracture networks in inter-pillow breccias, and enhanced by hydrofracturing due to the presence of seawater or hydrous minerals developed along such cracks (Staude et al., 2017).

Similar processes of sulfide infiltration may occur in deep-seated orebodies by injection of liquid sulfide into tectonically-generated tensional fractures (e.g. Figure 1C,D,F, Figure 14), including damage zones at the propagating tip of the host intrusion (Barnes and Mungall, 2018). We suggest that the close juxtaposition of brittle fracturing and soft-inclusion breccias, as seen at Savannah (Figure 14), is the result of transient high strain rates close to the brittle-ductile transition, reflecting thixotropic behaviour of hot silicate rock close to its solidus.

6.2. Magmatic sulfide matrix ore breccias

Based on detailed studies, primarily at Voisey's Bay and Aguablanca, we conclude that the main common feature in the origin of polymict magmatic sulfide matrix ore breccias is invasion of sulfide into pre-existing silicate-matrix intrusion breccias, the crucial line of evidence being the preservation of delicate crystal frameworks within sulfide between the inclusions. This process involves displacement of the original silicate matrix, either as existing melt, or by melting due to heat introduced with the sulfides.

The first step is the same as that in the formation of emulsion textures, i.e. mingling of immiscible sulfide and silicate melts due to detachment and diapirism of silicate melt films at magmatic contacts, and disaggregation of silicate rock inclusions due to melt film generation at grain boundaries close to hot sulfide liquid. Variable degrees of inclusion melting and disaggregation may have occurred during or before sulfide emplacement. Hard versus soft inclusion boundaries depend in most cases on the inclusion lithology. Inclusions with low melting temperatures, such as pelitic sediments or granitoids, tend to disaggregate along grain boundaries and disperse into sulfides, while lithologies with high melting temperatures, such as basalts or carbonates, tend to preserve sharp boundaries. The composition of the carrier melt (e.g. komatiitic or basaltic) also plays a role: the hotter sulfide liquid associated with komatiites is capable of melting basalt, as in the Moran example, whereas basaltic inclusions in mafic-hosted systems tend to be sharp-walled.

A characteristic of sulfide matrix ore breccias at Voisey's Bay and Aguablanca is the presence of refractory crystal assemblages enclosed within sulfide and apparently derived from an original silicate matrix component rather than from the inclusions; this is the plagioclase framework in the Voisey's Bay breccias (Figure 10). Barnes et al. (2017b) suggested that the presence of plagioclase-dominated inter-inclusion frameworks was a consequence of progressive displacement of the lower-melting temperature component of the silicate matrix; the eutectic multi-phase component melts first (or crystallises last) and is displaced by sulfide, leaving behind progressively fewer phases until a refractory monomineralic component remains (plagioclase at Voisey's Bay and pyroxene at Aguablanca). Transitional stages are recorded by the preservation of scattered sulfide-free oikocrysts of pyroxene or olivine, giving rise to the characteristic "leopard textures" reported at Voisey's Bay.

In this view, sulfide matrix ore breccias form by gravity-driven percolation of sulfide through the pore space of partially molten silicate rock, the same process that is believed to form interspinifex ore and much of the net-textured ore in komatiitic type 1 deposits (Barnes *et al.*, 2017d). The drivers are the high density, low viscosity and high heat capacity of sulfide liquid, allowing development of downward propagating finger instabilities against the opposing capillary force that arises from the stronger tendency of silicate melt rather than sulfide melt to wet solid silicate phases (Chung and Mungall, 2009, Saumur and Cruden, 2017).

This model raises the question of the how the intrusion breccias are formed in the first place. Barnes et al. (2016b) propose initial emplacement by gravity flow of xenolith-rich "sludge", possibly also containing sulfide, derived by wall and roof stoping at higher levels of sill-dyke networks (Figure 17). This process may have occurred during a late drain-back stage of magma emplacement as the magma flux through the intrusion network waned. Alternatively, it may represent a stage where the accumulated load of xenoliths, phenocrysts and sulfide droplets in an ascending suspension increased to the point where the suspension was no longer buoyant relative to the country rocks, resulting in a cessation of flow or a reversal of flow direction, and consequent choking of the conduit neck. In the case of Savannah, and other similar deposits hosted in bladed dykes, "sludge piles" of country rock fragments, endogenously derived fragments of host intrusion and assimilated sulfide may collapse from zones of wall-rock melting at the sides of the intrusion to accumulate at the bottom edge of a laterally propagating dyke (Barnes and Mungall, 2018). Subsequent gravity-driven drainage of the sulfide through the breccia porosity in any of these scenarios generates the observed ore textures.

Figure 17. Intrusion-ore genesis – percolation cartoon.

6.3. Tectonic breccias

Tectonic durchbewegung breccias reflect deformation of heterogeneous mixtures of weak, plastically deformable sulfide with strong, brittly-fracturing silicate rock, and may form under any circumstances where such mixtures are being sheared, stretched or compressed. Solid-state flow of sulfide into dilational veins, shear zones and pressure shadows during rock deformation takes place below the melting range, and in many cases below the temperature of exsolution of much of the pentlandite, accounting for observations of grain scale deformation microtextures within pentlandite grains, and lineations and foliations defined by crystallographic and shape preferred orientation of pyrrhotite and shape preferred orientation of elongate pentlandites (Vukmanovic, 2013, Vukmanovic *et al.*, 2014). Such textures are potentially diagnostic of tectonic breccias, but systematic observations are rare (McQueen, 1979, Cowden and Archibald, 1987). We offer a set of discrimination criteria for magmatic vs tectonic breccias in Table 3.

The most favourable setting for development of sulfide matrix durchbewegung breccias is where magmatic breccias exist in the first place, and particularly where these occupy either planar contacts or off-contact vein arrays. On the basis of a complete continuum of deformation intensity and inclusion populations as seen at Savannah (Figure 13), we suspect that most durchbewegung breccias in nickel sulfide deposits start life as magmatic breccias.

6.4. "Remobilised sulfides"

It is common practice in nickel sulfide mines and exploration projects to refer to any breccia-textured or vein-hosted sulfide as "remobilised", with the implication being that it has been moved by tectonic processes away from its original site of deposition. One of the central messages of this contribution is that, while tectonic dislocation or re-emplacement of sulfide bodies certainly can happen during deformation, it should not be automatically assumed that any sulfide ore mass lying outside its original host has necessarily been “remobilised”. In many of the cases illustrated here, the sulfide liquid invaded its floor or wall rocks at magmatic temperatures by essentially igneous processes that were an integral part of the primary ore-forming event. We recommend that the criteria for recognizing durchbewegung breccias should be applied before describing any sulfide body as “remobilised”, and that where these criteria are lacking, or ambiguous, then purely descriptive terminology should be used. This is critical to understanding orebody geometry during resource delineation: truly remobilized ores will have their geometry determined by the orientation of the stress field at the time of deformation, not at the time of emplacement, and consequently may bear no relationship to the geometry of the host igneous body.

6.5. Feedback in massive sulfide ore accumulation?

The textures we describe here and in the companion paper (Barnes *et al.*, 2017d) attest to magmatic sulfide liquids being remarkably aggressive natural fluids, possessing a combination of high temperatures, high heat capacity, high density and very low viscosity. These attributes combine to make percolating sulfide liquids extremely efficient carriers of heat and agents of melting of country rocks, particularly where sulfide liquids are able to invade pre-existing fractures (Saumur and Cruden, 2017). Staude et al (2016) expanded on a suggested by Groves et al. (1986) that sulfide liquids themselves, as much as the magmas that transport them, are major agents of thermomechanical erosion of country rocks. A pool or basal flow of sulfide liquid has the power to erode its own host embayment, through development of melting-infiltration fronts as seen at Moran; this property may account for the distinctive embayment and pinchout morphology of the Kambalda ore shoots. Hence a type of feedback may develop in mineral systems whereby an initial accumulation of sulfide deepens and enhances the trap site that originally formed it, thus making it a more effective trap for ongoing accumulation of sulfide from the flowing carrier magma. Self-organised, feedback-driven infiltration of sulfide melt into fractures in the footwall is a major driver of this process. Furthermore, sulfide that has invaded the country rock becomes insulated from further entrainment by flowing magma, enhancing its chances of preservation. This may be an important component of ore formation given the likelihood that sulfide liquid pools may be readily re-entrained by magma flowing over them (Robertson *et al.*, 2014, Barnes and Robertson, 2018), or may become unstable and flow back down the conduit system (Barnes et al. 2016b). This tendency of sulfide liquids to make their own trap sites and to drive the propagation of their own host intrusions may be a critical feedback loop in the development of magmatic sulfide mineral systems.

7. Conclusions

With the benefit of the detailed observations reported here, we expand on the classification scheme outline in Section 4 above in more systematic detail in Table 2. It should be born in mid that some critical features of sulfide-rich ores require outcrop or underground exposures for their identification, but such observations are commonly not available during exploration and drill-out. Hence the scheme proposed here is based largely on observable features of ores at hand sample or drill core scale.

Massive and semi-massive ores fall into five major categories (Table 2):

1. Pure inclusion-free massive sulfide ores;
2. Emulsion textured ores formed by frozen mixtures of molten silicate and sulfide, most commonly developed as melt films at thermal erosion contacts;
3. Sulfide matrix ore breccias, of sharp-wall, soft-wall or mixed character, developed by flooding of percolating sulfide matrix through the matrix of original silicate-melt-matrix intrusion breccias;
4. Vein-hosted sulfides formed at late magmatic or high temperature post-emplacement deformation stage close to the brittle-ductile transition in the country rocks or host igneous bodies; closely spaced intersecting vein arrays may produce the appearance of sulfide-matrix breccias in drill core;
5. Tectonic “durchbewegung” breccias, formed by mechanical inter-shearing of silicate inclusions and weak, ductile solid sulfides.

All gradations exist between these categories, and many examples of tectonic breccias may be tectonised versions of magmatic breccia precursors.

Sulfide matrix breccias form a continuum with various types of sulfide-poor silicate-rich ores, the common process being the gravity-driven infiltration of sulfide melt through the pore space of melting or still-molten substrate rocks. Sulfide melt infiltration links sulfide matrix ore breccias and emulsion textured ores with distinctive textures such as net-texture (matrix ore texture), leopard texture (poikilitic net texture) and interspinifex ore. In dynamic conduit systems, the process of gravity-driven sulfide migration at melting-infiltration fronts may give rise to a feedback where the sulfide magma erodes and deepens its own trap sites.

Acknowledgements

We are grateful to the following companies for allowing access to underground workings and drill core: Vale for Sudbury (Totten mine), Thompson and Voisey's Bay; Lundin Resources for Aguablanca and Eagle; IGO Ltd. for Long-Victor (Moran) and Nova; Cassini Resources for Nebo-Babel; Panoramic Resources for Savannah; MPI for Silver Swan; Noril'sk Nickel for Okyabrysky; and Western Areas for Spotted Quoll. We thank the organizers and field trip guidebook editors of the 2014 International Platinum Conference in Russia for permission to use the image in Figure 2B. The synchrotron X-ray fluorescence maps were collected on the X-ray fluorescence microscopy beamline at the Australian Synchrotron, Clayton, Victoria, Australia, and we acknowledge the assistance of Daryl Howard and David Paterson of ANSTO. We further acknowledge financial support for this facility from the Science and Industry Endowment Fund (SIEF). Michael Verrall provided essential support for the Tornado microbeam XRF mapping and X-ray tomography. Additional samples from Aguablanca and helpful discussions were provided by Nick Arndt and Steve Beresford. Valentina Taranovic helped improve an earlier version of the manuscript. SJB and MLV were financially supported by fellowships from the CSIRO Research Plus Office (formerly Office of the Chief Executive).

============================

Additional references from tables for Endnote (*to be deleted in final copy*): (Staude *et al.*, 2016, Staude *et al.*, 2017a, Staude *et al.*, 2017b) (Dowling *et al.*, 2004) (Barnes *et al.*, 2017b) Likhachev (Godlevsky and Likhachev, 1986, Likhachev, 1994) (Casquet *et al.*, 2001, Ortega *et al.*, 2004, Tornos *et al.*, 2006, Pina *et al.*, 2010) (Lightfoot *et al.*, 2017) (Prichard *et al.*, 2013)

===

References

Barnes S.J., Beresford S.W., Le Vaillant M., 2016a, Interspinifex Ni sulfide ore from the Coronet Shoot, Kambalda: characterisation using microbeam XRF mapping and 3D X-ray computed tomography. Economic Geology, 111, 1509-17: 10.2113/econgeo.111.6.1509.

Barnes S.J., Cruden A.R., Arndt N.T., Saumur B.M., 2016b, The mineral system approach applied to magmatic Ni-Cu-PGE sulphide deposits. Ore Geology Reviews, 76, 296-316: 10.1016/j.oregeorev.2015.06.012.

Barnes S.J., Holwell D.A., Le Vaillant M., 2017a, Magmatic sulfide ore deposits. Elements, 13, 91-7: 10.2113/gselements.13.2.91

Barnes S.J., Hutchison N., Warriner S. 2017b, Black Swan nickel sulfide deposits. In: Phillips N, editor. Australian Ore Deposits Monograph. Melbourne: Australian Institute of Mining and Metallurgy; p. 123-6.

Barnes S.J., Le Vaillant M., Lightfoot P.C., 2017c, Textural development in sulfide-matrix ore breccias and associated rocks in the Voisey's Bay Ni-Cu-Co deposit, Labrador, Canada. Ore Geology Reviews, 90, 414-38: 10.1016/j.oregeorev.2017.03.019.

Barnes S.J., Mungall J.E., 2018, Blade shaped dykes and nickel sulfide deposits: a model for the emplacement of ore-bearing small intrusions. Economic Geology, in press.

Barnes S.J., Mungall J.E., Le Vaillant M., Godel B., Lesher C.M., Holwell D.A., Lightfoot P.C., Krivolutskaya N.A., Wei B., 2017d, Sulfide-silicate textures in magmatic Ni-Cu-PGE sulfide ore

deposits: Disseminated and net-textured ores. AMERICAN MINERALOGIST, 102, 473-506: 10.2138/am-2017-5754.
Barnes S.J., Pina R., Le Vaillant M., 2018, Textural development in sulfide-matrix ore breccias in the Aguablanca Ni-Cu deposit, Spain, revealed by X-ray fluorescence microscopy. Ore Geology Reviews, online: 10.1016/j.oregeorev.2018.03.004.
Barnes S.J., Robertson J.C., 2018, Time scales and length scales in magma flow pathways and the origin of magmatic Ni-Cu-PGE ore deposits. Geoscience Frontiers, in press.
Casquet C., Galindo C., Tornos F., Velasco F., Canales A., 2001, The Aguablanca Cu-Ni ore deposit (Extremadura, Spain), a case of synorogenic orthomagmatic mineralization: age and isotope composition of magmas (Sr, Nd) and ore (S). Ore Geology Reviews, 18, 237-50.
Chung H.-Y., Mungall J.E., 2009, Physical constraints on the migration of immiscible fluids through partially molten silicates, with special reference to magmatic sulfide ores. Earth and Planetary Science Letters, 286, 14-22.
Cowden A., Archibald N.J., 1987, Massive-sulfide fabrics at Kambalda and their relevance to the inferred stability of monosulfide solid-solution. Canadian Mineralogist, 25, 37-50.
Craig J.R., Kullerud G., 1969, Phase relations in the Cu-Fe-Ni-S system and their application to magmatic ore deposits. Economic Geology Monograph, 4, 344-58.
Ding X., Ripley E.M., Li C.S., 2012a, PGE geochemistry of the Eagle Ni-Cu-(PGE) deposit, Upper Michigan: constraints on ore genesis in a dynamic magma conduit. Mineralium Deposita, 47, 89-104.
Ding X., Ripley E.M., Shirey S.B., Li C., 2012b, Os, Nd, O and S isotope constraints on country rock contamination in the conduit-related Eagle Cu-Ni-(PGE) deposit, Midcontinent Rift System, upper Michigan. Geochimica et Cosmochimica Acta, 89, 10-30.
Dowling S.E., Barnes S.J., Hill R.E.T., Hicks J., 2004, Komatiites and Nickel Sulfide Ores of the Black Swan area, Yilgarn Craton, Western Australia. 2. Geology and Genesis of the Orebodies. Mineralium Deposita, 39, 707-28.
Evans-Lamswood D.M., Butt D.P., Jackson R.S., Lee D.V., Muggridge M.G., Wheeler R.I., Wilton D.H.C., 2000, Physical controls associated with the distribution of sulfides in the Voisey's Bay Ni-Cu-Co deposit, Labrador. Economic geology and the Bulletin Of the Society Of Economic Geologists, 95, 749.
Frost K.M., Groves D.I., 1989, Magmatic contacts between immiscible sulfide and komatiitic melts; implications for genesis of Kambalda sulfide ores. Economic Geology, 84, 1697-704.
Godel B., Barnes S.J., Barnes S.-J., 2013, Deposition mechanisms of magmatic sulphide liquids: evidence from high-resolution X-ray computed tomography and trace element chemistry of komatiite-hosted disseminated sulphides. Journal of Petrology, 54, 1455-81: 10.1093/petrology/egt018.
Godlevsky M.N., Likhachev A.P. 1986, Types and distinctive features of ore-bering formations of copper-nickel deposits. In: Friedrich GH, Genkin AD, Naldrett AJ, Ridge JD, Sillitoe RH, Vokes FM, editors. Heidelberg: Springer Verlag; p.
Groves D.I., Korkiakoski E.A., McNaughton N.J., Lesher C.M., Cowden A., 1986, Thermal erosion by komatiites at Kambalda, Western Australia and the genesis of nickel ores. Nature, 319, 136-9.
Hawley J., 1962, The Sudbury ores, their mineralogy and origin; Part 1, The geological setting, . Canadian Mineralogist, 7, 1-29.
Hicks, J., Barnes S.J., Le Vaillant M., Mole D. 2017, Savannah nickel sulfide deposits. In: Phillips N, editor. Australian Ore Deposits Monograph. Melbourne: Australian Institute of Mining and Metallurgy; p. 435-40.
Hoatson D.M., Blake D.H. Geology and economic potential of the Palaeoproterozoic layered mafic-ultramafic intrusions in the East Kimberley, Western Australia. AGSO Bulletin Canberra: Australian Geological Survey Organisation; 2000. p. 476.
Keays R.R., Lightfoot P.C., 2015, Geochemical Stratigraphy of the Keweenawan Midcontinent Rift Volcanic Rocks with Regional Implications for the Genesis of Associated Ni, Cu, Co, and Platinum

Group Element Sulfide Mineralization Economic Geology, 110, 1235-67: 10.2113/econgeo.110.5.1235.
Kohanpour F., Gorczyk W., Lindsay M.D., Occhipinti S.A., 2017, Examining tectonic scenarios using geodynamic numerical modelling: Halls Creek Orogen, Australia. Gondwana Research, 46, 95-113.
Le Vaillant M., Barnes S.J., Mungall J.E., Mungall E., 2017, Role of de-gassing of the Noril'sk nickel deposits in the Permo-Triassic mass extinction event. Proceedings of the National Academy Of Sciences, 114, 2485-90: 10.1073/pnas.1611086114.
Lesher C.M., Keays R.R. 2002, Komatiite-associated Ni-Cu-PGE deposits: geology, mineralogy, geochemistry and genesis. In: Cabri LJ, editor. The Geology, Geochemistry Mineralogy and Mineral Beneficiation of Platinum Group Elements: Canadian Institute of Mining Metallurgy and Petroleum Special Volume 54; p. 579-617.
Li C., Naldrett. 2000, Melting reactions of gneissic inclusions with enclosing magma at Voisey's Bay, Labrador, Canada; implications with respect to ore genesis. Economic geology and the Bulletin Of the Society Of Economic Geologists, 95, 801-14.
Lightfoot P.C. 2016,Nickel Sulfide Ores and Impact Melts: Elsevier.
Lightfoot P.C., Keays R.R., Evans-Lamswood D., Wheeler R., 2012, S saturation history of Nain plutonic suite mafic intrusions; origin of the Voisey's Bay Ni-Cu-Co sulfide deposit, Labrador, Canada. Mineralium Deposita, 47, 23-50: http://dx.doi.org/10.1007/s00126-011-0347-6.
Lightfoot P.C., Stewart R., Gribbin G., Mooney S.J., 2017, Relative contribution of magmatic and post-magmatic processes in the genesis of the Thompson Mine Ni-Co sulfide ores, Manitoba, Canada. Ore Geology Reviews, 83, 258-86.
Lightfoot P.C., Zotov I.A., 2014, Geological relationships between the intrusions, country rocks and Ni-Cu-PGE sulfides of the Kharealakh Intrusion, Noril'sk region: Implications for the role of sulfide differentiation and metasomatism in their genesis. Northwestern Geology, 47, 1-35.
Likhachev A.P. 1994, Ore-bearing intrusions of the Noril'sk region. In: Lightfoot PC, Naldrett AJ, editors. Proceedings of the Sudbury-Noril'sk Symposium Ontario Geological Survey Special Publication 5: Ontario Geological Survey, Toronto, ON; p. 185-201.
Mariga J., Ripley E.M., Li C., 2006a, Oxygen isotopic studies of the interaction between xenoliths and mafic magma, Voisey's Bay Intrusion, Labrador, Canada. Geochimica et Cosmochimica Acta, 70, 4977-96: http://dx.doi.org/10.1016/j.gca.2006.07.018.
Mariga J., Ripley E.M., Li C., 2006b, Petrologic evolution of gneissic xenoliths in the Voisey's Bay Intrusion, Labrador, Canada: Mineralogy, reactions, partial melting, and mechanisms of mass transfer. Geochemistry, Geophysics, Geosystems, 7: 10.1029/2005GC001184.
McQueen K.G., 1979, Experimental heating and diffusion effects in Fe-Ni sulphide ore from Redross, Western Australia. Economic Geology, 74, 140-8.
Mudd G.M., Jowitt S.M., 2014, A Detailed Assessment of Global Nickel Resource Trends and Endowments. Economic Geology, 109, 1813-41.
Naldrett A.J., 1969, A portion of the system Fe-S-O and its application to sulfide ore magmas. Journal of Petrology, 10, 171-202.
Naldrett A.J., 1997, Key Factors In The Genesis Of Norilsk, Sudbury, Jinchuan, Voiseys Bay And Other World-Class Ni-Cu-Pge Deposits - Implications For Exploration. Australian Journal of Earth Sciences, 44, 283-315.
Naldrett A.J. 2004,Magmatic Sulfide Deposits: Geology, Geochemistry and Exploration. Heidelberg: Springer.
Naldrett A.J., Keats H., Sparkes K., Moore R., 1996, Geology of the Voisey's Bay Ni-Cu-Co deposit, Labrador, Canada. EXPLORATION AND MINING GEOLOGY, 5, 69-179.
Ortega L., Lunar R., Garcia-Palomero F., Moreno T., Martin-Estrevez J.R., Prichard H.M., Fisher P.C., 2004, The Aguablanca Ni-Cu-Pge Deposit, Southwestern Iberia: Magmatic Ore-Forming Processes and Retrograde Evolution. Canadian Mineralogist, 42, 325-50.
Peck D.C., Huminicki M.A.E., 2016, Value of mineral deposits associated with mafic and ultramafic magmatism: Implications for exploration strategies. Ore Geology Reviews, 72, 269-98.

Piña R., Lunar R., Ortega L., Gervilla F., Alapieti T., Martinez C., 2006, Petrology and Geochemistry of Mafic-Ultramafic Fragments From the Aguablanca Ni-Cu Ore Breccia, Southwest Spain. Economic Geology, 101, 865-81.
Pina R., Romeo I., Ortega L., Lunar R., Capote R., Gervilla F., Tejero R., Quesada C., 2010, Origin and emplacement of the Aguablanca magmatic Ni-Cu-(PGE) sulfide deposit, SW Iberia; a multidisciplinary approach. GEOLOGICAL SOCIETY OF AMERICA BULLETIN, 122, 915-25: http://dx.doi.org/10.1130/B30046.1.
Prichard H.M., Fisher P.C., McDonald I., Knight R.D., Black A.P., Sharp D.R., Williams J.P., 2013, The distribution of PGE and the role of arsenic as a collector of PGE in the Spotted Quoll nickel ore deposit in the Forrestania Greenstone Belt, Western Australia. Economic Geology, 108, 1903-21.
Ripley E.M., Li C. 2011, A Review of Conduit-Related Ni-Cu-(PGE) Sulfide Mineralization at the Voisey's Bay Deposit, Labrador, and the Eagle Deposit, Northern Michigan. In: Li C, Ripley EM, editors. Magmatic Ni-Cu and PGE deposits: geology, geochemistry and genesis Reviews in Economic Geology 17. Littleton: Society of Economic Geologists; p. 181-97.
Robertson J.C., Barnes S.J., Metcalfe G. Chaotic entrainment can drive sulfide remobilization at low magma flow rates. 13th International Platinum Symposium. Yekaterinburg, Russia: Russian Academy of Sciences, Ural Branch; 2014. p. 47-8.
Ryan B., 2000, The Nain-Churchill boundary and the Nain plutonic suite: A regional perspective on the geologic setting of the Voisey's Bay Ni-Cu-Co deposit. Economic geology and the Bulletin Of the Society Of Economic Geologists, 95, 703- 24.
Saumur B.M., Cruden A.R., 2016, On the emplacement of the Voisey's Bay intrusion (Labrador, Canada). GEOLOGICAL SOCIETY OF AMERICA BULLETIN, 128, 147-68: 10.1130/B31240.1.
Saumur B.M., Cruden A.R., 2017, Ingress of magmatic Ni-Cu sulphide liquid into surrounding brittle rocks: physical & structural controls. Ore Geology Reviews, online: http://dx.doi.org/10.1016/j.oregeorev.2017.06.009.
Saumur B.M., Cruden A.R., Evans-Lamswood D.M., Lightfoot P.C., 2015, Wall-Rock Structural Controls on the Genesis of the Voisey's Bay Intrusion and its Ni-Cu-Co Magmatic Sulfide Mineralization (Labrador, Canada). Economic Geology, 110, 691-711: 10.2113/econgeo.110.3.691
Sluzhenikin S.F., Krivolutskaya N.A., Rad'ko V., Malitch K.N., Distler V.V., Fedorenko V.A. 2014,Ultramafic-mafic intrusions, volcanic rocks and PGE-Cu-Ni sulfide deposits of the Noril'sk Province, Polar Siberia, Field Trip Guidebook. Yekaterinburg, Russia.: Institute of Geology of Ore Deposits, Petrography, Mineralogy and Geochemistry.
Staude S., Barnes S.J., Le Vaillant M., 2016, Evidence of lateral thermomechanical erosion of basalt by Fe-Ni-Cu sulfide melt at Kambalda, Western Australia. Geology, 12, 1047-50: 10.1130/G37977.1.
Staude S., Barnes S.J., Le Vaillant M., 2017a, Thermomechanical excavation of ore-hosting embayments beneath komatiite lava channels: textural evidence from the Moran deposit, Kambalda, Western Australia. Ore Geology Reviews, 90, 446-64: 10.1016/j.oregeorev.2017.05.001.
Staude S., Sheppard S., Parker P., Paggi J. 2017b, Long-Victor nickel sulfide complex, Kambalda, Western Australia. In: Phillips N, editor. Australian Ore Deposits Monograph. Melbourne: Australian Institute of Mining and Metallurgy; p.
Tornos F., Casquet C., Galindo C., Velasco F., Canales A., 2001, A new style of Ni-Cu mineralization related to magmatic breccia pipes in a transpressional magmatic arc, Aguablanca, Spain. Mineralium Deposita, 36, 700-6.
Tornos F., Galindo C., Casquet C., Pevida L.R., Martinez C., Martinez E., Velasco F., Iriondo A., 2006, The Aguablanca Ni-(Cu) sulfide deposit, SW Spain; geologic and geochemical controls and the relationship with a midcrustal layered mafic complex. Mineralium Deposita, 41, 737-69: http://dx.doi.org/10.1007/s00126-006-0090-6.
Vukmanovic Z., 2013. Microstructural characterization of sulphide and oxide minerals in magmatic sulphide ores. Nedlands: University of Western Australia. p. Pages.

Vukmanovic Z., Reddy S.M., Godel B., Barnes S.J., Fiorentini M.L., Barnes S.-J., Kilburn M.R., 2014, Relationship between microstructures and grain-scale trace element distribution in komatiite-hosted magmatic sulphide ores. Lithos, 184-187, 42-61: 10.1016/j.lithos.2013.10.037.

Figure captions

Figure 1. Underground face and wall photographs showing hard inclusion breccias and sulfide breccia veins at cm-dm scale. A, B, Savannah. Sulfide matrix breccias with primarily sharp-walled inclusions, commonly showing evidence of mild folding; inclusion populations are mafic granulite and metasedimentary gneisses plus fine grained norite from host intrusion. C, Nova, Western Australia, combination of sharp-walled sulfide vein arrays with breccias containing mildly deformed inclusions of immediate mafic granulite country rock. D, Savannah, wall rock fragments (ultramafic cumulates) within dispersed, irregular sulfide-filled vein array.

Figure 2. Underground face (A-D) and core (E) photographs showing silicate-sulfide melt emulsions and soft-wall inclusion breccias developed at melting-infiltration fronts beneath massive sulfide pools. A, McLeay Shoot, Long-Victor Mine, Kambalda: transition from silicate-sulfide emulsions in top ~10 cm into monomict sulfide matrix breccia with basalt inclusions in dense interconnected sulfide vein network. B. Base of Cu-rich massive sulfide at the Oktyabrsky Mine, Talnakh, Siberia, showing sulfide injection along bedding planes in footwall argillite and partially detached fragments of argillite peeling away from the floor and ascending into melt. Photo courtesy of N. Krivolutskaya, S. Sluzhenikin and field trip leaders of the Noril'sk excursion at the 13th International Platinum Symposium; photo from the field trip guidebook (Sluzhenikin et al, 2014). D, E (sulfide in red, dacite footwall unit in grey in D): sulfide liquid fills fractures in dacite, dacite inclusions in sulfide are a connected framework of partially molten buoyantly ascending “blobs” rising into sulfide melt. E, detail of a plume of dacite melt still attached to the floor.

Figure 3. Detail of silicate-sulfide emulsion-textured ores. A,B: “type sample” from Frood-Stobie mine, Sudbury described by Hawley (1962). Globular inclusions of quartz diorite within sulfide matrix. B is a false-colour microbeam XRF element distribution map collected using the Bruker Tornado microbeam XRF mapper (henceforth “Tornado maps”); sulfides in yellow-brown, silicates in green. Note fine rind of enrichment in Cr-spinel (blue-green) developed around some of the silicate globules, enlarged in D, and feathery “quench textures” within inclusions (C). E, emulsion textured ore from Moran, Kambalda, showing zoned globules of original basalt melt with chromite rinds (blue-green) in sulfide matrix, in identical texture to that in A,B. F, globule of quench-textured Mg-dolerite showing microspinifex cpx texture within sulfide, Aguablanca deposit. G, Kharealakh intrusion, Talnakh, Siberia, swirled globules of granophyric melt within sulfide. H, stretched and swirled globules of dacite melt within sulfide, Silver Swan deposit.

Figure 4. Moran: Infiltration-melting front at basal contact of massive sulfide orebody, Moran Shoot, Kambalda. A,C,D and F are Tornado XRF element maps (3-element false colour images for A, C and D, single-element greyscale image for Cr abundance in F). A, drill core through basal contact showing transition from melt emulsion with fine chromite (red) rims at silicate–sulfide melt contacts, to crackle breccia with sulfide($) invading fractures in original basalt (B) flow top. B, C: ascending basalt plumes into sulfide at basal contact; dendritic chromite (red) forms clusters nucleating on basalt melt contacts and growing into sulfide. D, sulfide (black) invading bedded aluminous cherty sediment, giving rise to alternating bands of unmelted quartz-rich refractory sediment with fine emulsion texture developed within more calcic bands. E, underground face photograph showing

basalt melt plume ascending into sulfide from banded, originally horizontal melt film layer (lower right). F, skeletal chromite developed within sulfide ($) at basalt melt (BM) contact.

Figure 5. Moran. Silicate-sulfide emulsion textures formed by accumulation of “floating” silicate melt at the roof of a lateral “pinchout” structure. A, Tornado XRF element map of a cut slab from an underground ore face, showing sulfide overlain by a fine emulsion of sulfide and silicate melt, the latter now replaced by fine intergrowth of tremolite, chlorite and calcite. Chromite enriched band (red) developed at a plumose interface due to tendency of chromite to sink in the sulfide. B, polished slab, intercalated sulfide rich and poor bands at the accumulation interface, sulfide-poor band comprised of intergrown actinolite/tremolite and ferrian chromite; shown enlarged in C (reflected light photomicrograph). D, synchrotron-Maia XFM element map showing skeletal pyroxene now replaced by actinolite and fine feathery Fe-chromite (Chr) in matrix of pentlandite and pyrrhotite. Inset shows schematic of distribution of textural associations within the pinchout, modified from Staude et al. (2016, 2017).

Figure 6. “Inverted net texture”, a variant of emulsion textured ores formed where silicate melt is present where the sulfide has partially solidified to form subhedral “cumulus” monosulfide solid solution (MSS) crystals; silicate melt (usually hydrous or Si-rich or both) occupies the interstices between the MSS grains. A, Silver Swan (dacite melt); B, Moran, siliceous metasediment melt, same setting as that illustrated in Fig. 4D; C, Nebo-Babel, silicate melt derived by melting of country rock granite inclusions generating K-feldspar-quartz granophyre (red-yellow) enclosing aggregates of subhedral MSS grains.

Figure 7. Schematic geological reconstructions showing the disposition of sulfide matrix breccias and other ore types in relation of the geometry of the host intrusion. See Table 1 for sources. $ = sulfide, Dissem = disseminated; Mass = massive, inclusion free; SMOB = sulfide-matrix ore breccia; V = veins; Troc = troctolite, Gb = gabbro, Gno=gabbronorite, UM cmlt = ultramafic cumulate.

Figure 8. Eagle deposit, Michigan. Underground drive walls (A-C) and cut slabs of a sulfide-shale melt infiltration – emulsion contact. A, top and bottom contact of a ~2m thick massive sulfide sill injecting laterally along bedding planes of country rock black shales (Proterozoic Michigamme Formation). Note the planar top contact (upper right), compared with the basal contact where sulfide has injected along bedding planes causing shale layers to deflect upward at the trailing edge of the sulfide injection and melt at the sulfide contacts. B, C, details of sulfide-shale contact at base of sulfide, showing soft-inclusion breccia and emulsion textures formed by partial to complete melting of shale and detachment of melt plumes and blobs from the contact melt film into the sulfide. Note pre-ore pyrite-rich layer within the shale just below the contact in C. D, E, cut slab and Tornado XFM map of a sample collected from the same melt-film contact. Note stellate aggregates of elongate K-feldspar crystals in E indicating complete melting followed by rapid recrystallization of shale melt.

Figure 9. Sulfide matrix breccia ores from Sudbury. A, Contact style mineralization comprising massive sulfide with inclusions, Creighton Mine; B, Durchbewegung style sulfides in shear zone from Garson Mine footwall; C, Offset style primary sulfide breccia from Totten Mine on the Worthington Offset (see also Fig. 1E,F).

Figure 10. Sulfide matrix ore breccias from the Ovoid and Eastern Deeps, Voisey’s Bay, modified from Barnes et al. (2017c). A, polished slab of inclusion supported sulfide matrix breccia showing inclusions of felspathic peridotite (Um), consisting of olivine orthocumulate with interstitial plagioclase and clinopyroxene, and hercynite-anorthite paragneiss (HyPGn). Plagioclase laths (dark grey) form outgrowths on inclusions, extending into sulfide-rich domains; inset is Tornado map

showing detail of plag (Pl1) intergrowth with sulfide, and internal banding with paragneiss inclusions defined by abundance of skeletal hercynite (Hy) after corundum. B-E, Summary of textures of olivine gabbro or troctolite, in relation to the independent variables of sulfide content (increasing top to bottom row) and proportion of inclusions in the breccias (increasing left to right). Clasts are shown in plain grey to emphasize the textures in the sulfide-silicate matrix. Note the persistence of the plagioclase lath framework through the entire array and the disappearance of clinopyroxene in the most sulfide rich sample (E). Images are phase maps derived from Tornado XRF maps. Animated 3D tomography image of sample shown in frame A available at https://www.youtube.com/watch?v=hUGN9Lvt-08.

Figure 11. Aguablanca: silicate and sulfide matrix breccias. A. Silicate matrix breccia from upper margin of the intrusion, sharp-walled calc-silicate (marble) inclusions within heterogeneous "taxitic" gabbro. B, sulfide matrix ore breccia with hard-walled and soft-wall inclusions of pyroxenite and anorthosite; note disaggregation of some inclusions into "cloud" of pyroxene crystals within sulfide. Photos A, B from Lundin Mining. C, typical sulfide matrix breccia sample AB-NA1, disaggregating composite anorthositic gabbro - pyroxenite inclusions with soft disaggregating rims in sulfide, phase map derived from Tornado XRF map. Note preferential incorporation of pyroxene grains (arrowed) within former MSS (now pyrrhotite/pentlandite) compared with chalcopyrite. D, Tornado XRF map, inclusion-rich sulfide-matrix breccia, mainly calc-silicate inclusions, interconnected sulfide patches invading porphyritic gabbro disaggregating into sulfide-pyroxene cloud. E, Tornado map showing detail of inclusion margin in upper right of image C, disaggregating pyroxene-rich rim on anorthosite inclusion core; note presence of concentric oscillatory zoning in Cr (arrowed) in pyroxene grains in the inclusion margin and also embedded in sulfide. F, Synchrotron Maia image showing detail of Cr zoning in clinopyroxene.

Figure 12. Calc-silicate inclusions in sulfide matrix ore breccia, Oktyabrysky mine, Talnakh. Samples from underground exposure at contact between main contact massive ore and flanking calc-silicate unit. A, underground face, back of ore drive, zoned hard-contact calc-silicate fragments in inclusion rich sulfide with diffuse oxide-silicate patches. B-F, images of single hand sample from same locality: B, polished slab, reflected light; C-F synchrotron Maia XFM element maps of an entire thin section cut from same slab. Note complete replacement of original carbonate inclusion by wollastonite (Wo), with minor relic calcite (Cct) associated with anhydrite (Anh) in matrix of sulfide and magnetite (Mgt). Note that magnetite defines reaction rinds around inclusions that are slightly and regularly displaced into the sulfide from the edges of the inclusions. F, detail of E showing typical pentlandite (Pn) – pyrrhotite exsolution in two generations – coarse grain boundary exsolution forming "loop" texture, later lamellae in core of Po grains. Chlacopyrite (Ccp) within sulfide and locally replacing inclusions.

Figure 13. Savannah. Polished drill core slabs and false colour Tornado XFM maps (and derived phase maps) of Savannah sulfide matrix ore breccias showing polymict nature of breccias, mineralogically zoned inclusions, disaggregation along crystal boundaries and transition to durchbewegung textures. A, B: breccia with inclusions of garnet-rich paragneiss showing garnet-depleted, plagioclase enriched rims, a band of disaggregated plagioclase (lower region); no evident foliation although a band of pentlandite wraps around the central garnet-rich inclusion. C,D, breccia containing inclusions of fine igneous textured micronorite probably derived from the contact zone of the host intrusion, and inclusion of tonalite; note that one of the norite inclusions (lower) is itself a breccia containing a inclusion of microgranite. E, F, breccia containing inclusions of garnet-biotite gneiss with garnet rich rims (contrast A,B), a K-rich microgabbro or diorite probably derived from the country rock sequence; and a folded quartz-biotite schist showing marginal disaggregation; note incipient

development of foliation defined by quartz and biotite crystals and exsolved pentlandite. G,H,I: strongly foliated and folded durchbewegung (tectonically modified) breccia with folded biotite-rich inclusions, rigid undeformed inclusion of tonalite (lower left); note pronounced foliation developed by the sulfide minerals as well as the silicate inclusions.

Figure 14. Savannah mine, 1540 level. Probable tectonic or extreme late magmatic mobilisation of sulfide into parallel tension-vein array in immediate footwall of soft-wall sulfide matrix breccia ore. Note prominent vein (centre right, red arrow) cutting a pre-existing inclusion. Inset shows enlargement of propagating tip of fracture array; these fine vein tips are occupied primarily by chalcopyrite, rest of vein array is po>pn=ccp. “Down” indicates inferred primary stratigraphic orientation.

Figure 15. Tectonic breccias. A, B, Durchbewegung breccia from Thompson, Manitoba, Canada – quartz-rich metasediment inclusions in matrix of sulfide, pronounced planar fabric defined by pentlandite exsolving along preferred pyrrhotite orientation (foliation). C,D, sulfidic mylonite, Spotted Quoll deposit, Forrestania Greenstone Belt, Western Australia. Similar strong alignment of pyrrhotite foliation and exsolved pentlandite, strong planar alignment of silicate inclusions.

Figure 16. Cartoon showing development of emulsion textures and vein array breccia at a sulfide melt-infiltration front at the sulfide-basalt contact in the Moran embayment, Kambalda. A: Due to its high density and low viscosity the sulfide melt is able to exploit and infill an existing fracture network. B: Fluids of the hydrated basalt are released due to the high temperature; creates a network of microfractures accelerating the infiltration of sulfide and efficient heating of basalt. Clasts closer to the sulfide melt start to melt. The uppermost basalt inclusions are completely molten and form emulsions and plumes. Chromite grows on the contact between the basalt and sulfide melts. Modified from Staude et al., 2017a.

Figure 17. Stages in the development of a stylised magmatic Ni-Cu-(PGE) deposit within a dynamic sill-dyke conduit system (inset, top left) in the mid to upper crust, modified from Barnes et al. (2016b). Magma flow through the system is dominantly lateral and upward, interspersed with periods of backflow during hiatus in magma supply, and episodic gravity flow of dense sulfide melt or sulfide-silicate slurries. Inset in bottom right shows stage in the flooding of an original silicate-matrix intrusion breccia by downward percolating sulfide liquid, modified from Barnes et al. (2017c), giving rise to sulfide matrix ore breccias.

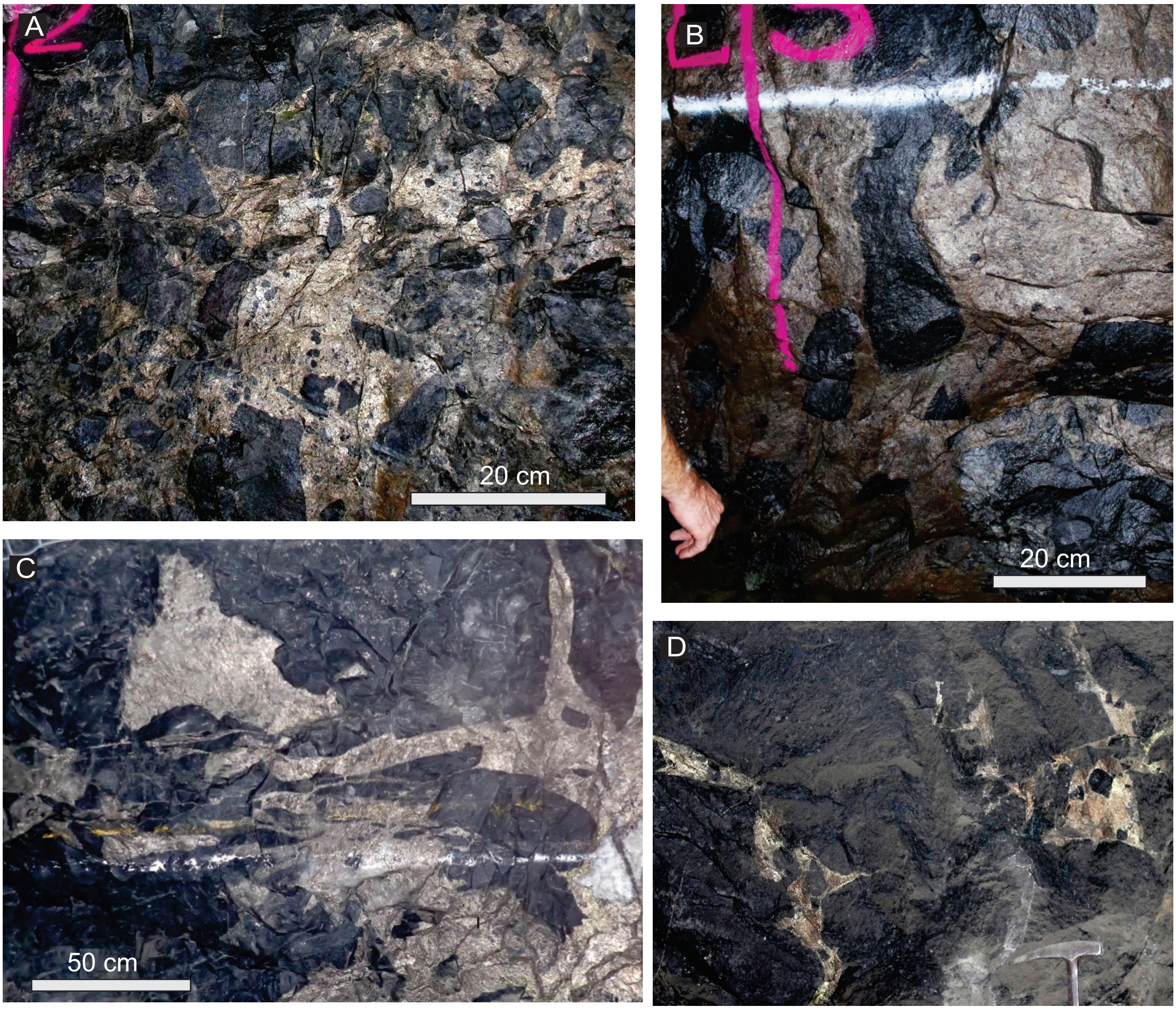
A
20 cm
B
20 cm
C
50 cm
D

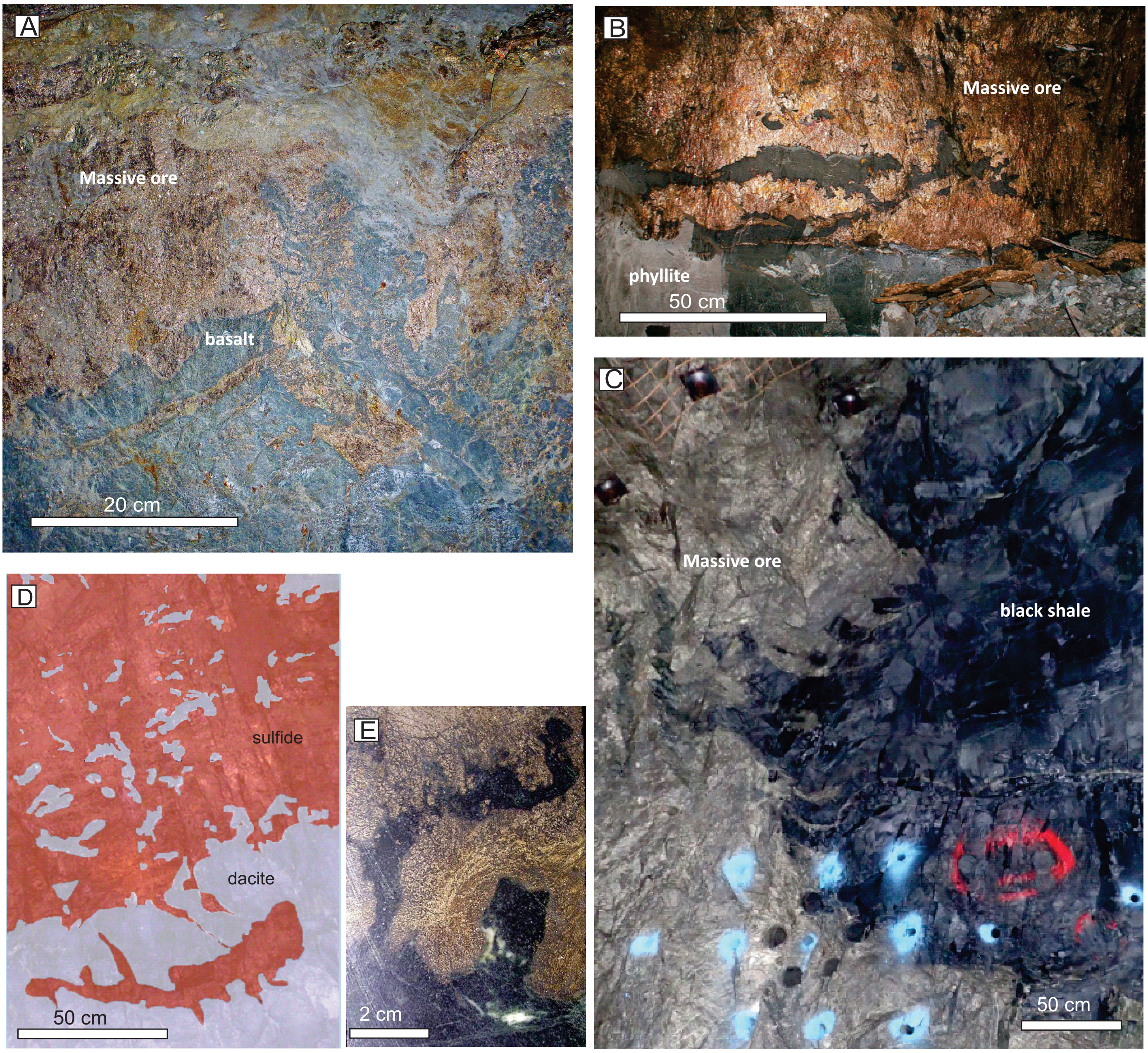
A
Massive ore
basalt
20 cm
B
Massive ore
phyllite
50 cm
C
Massive ore
black shale
50 cm
D
sulfide
dacite
50 cm
E
2 cm

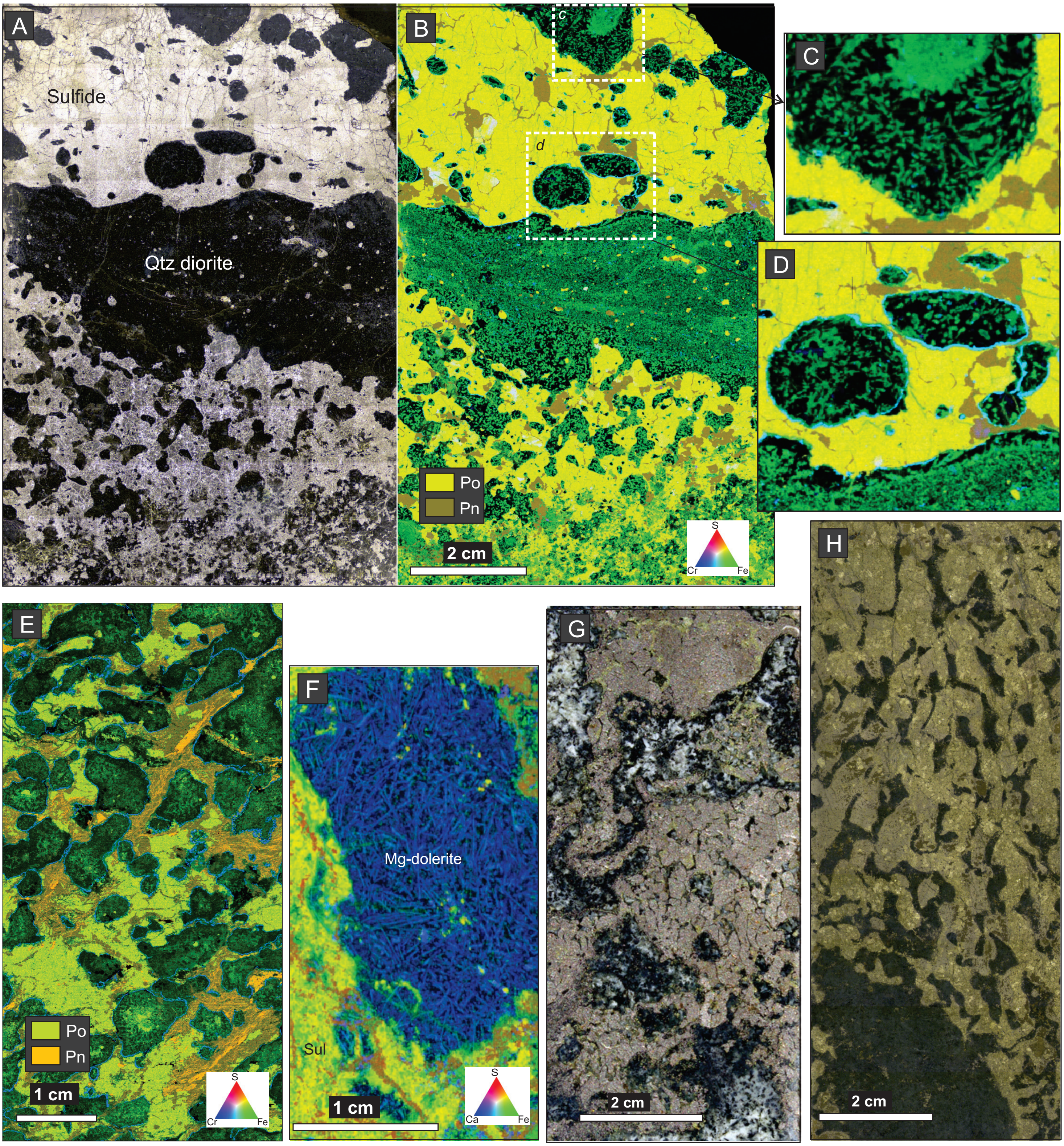

A
Sulfide
Qtz diorite
B
c
d
Po
Pn
2 cm
S
Cr
Fe
C
D
E
Po
Pn
1 cm
S
Cr
Fe
F
Mg-dolerite
Sul
1 cm
S
Ca
Fe
G
2 cm
H
2 cm

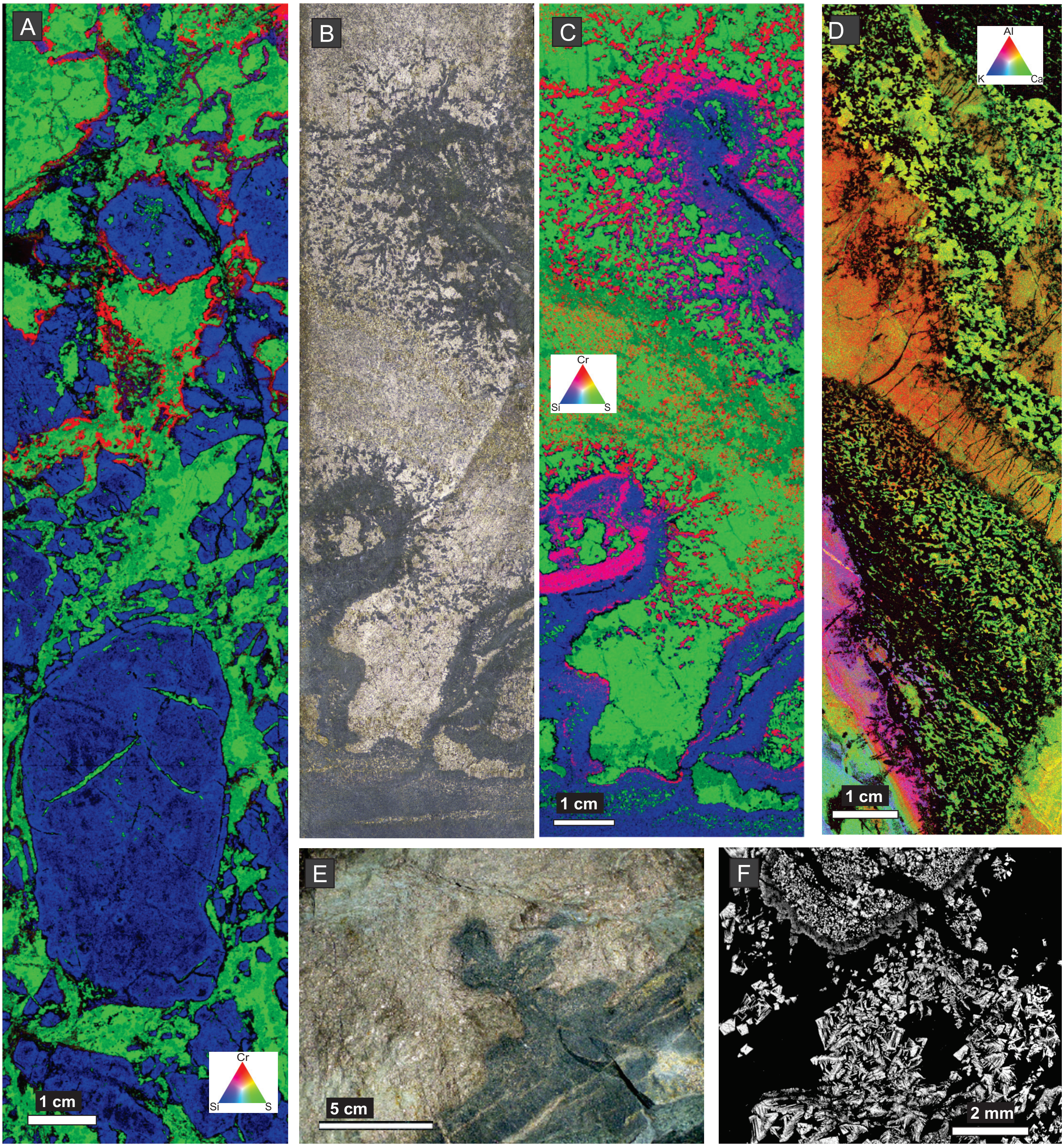
A
B
C
D
E
F
Cr
Si
S
Al
K
Ca
1 cm
5 cm
2 mm

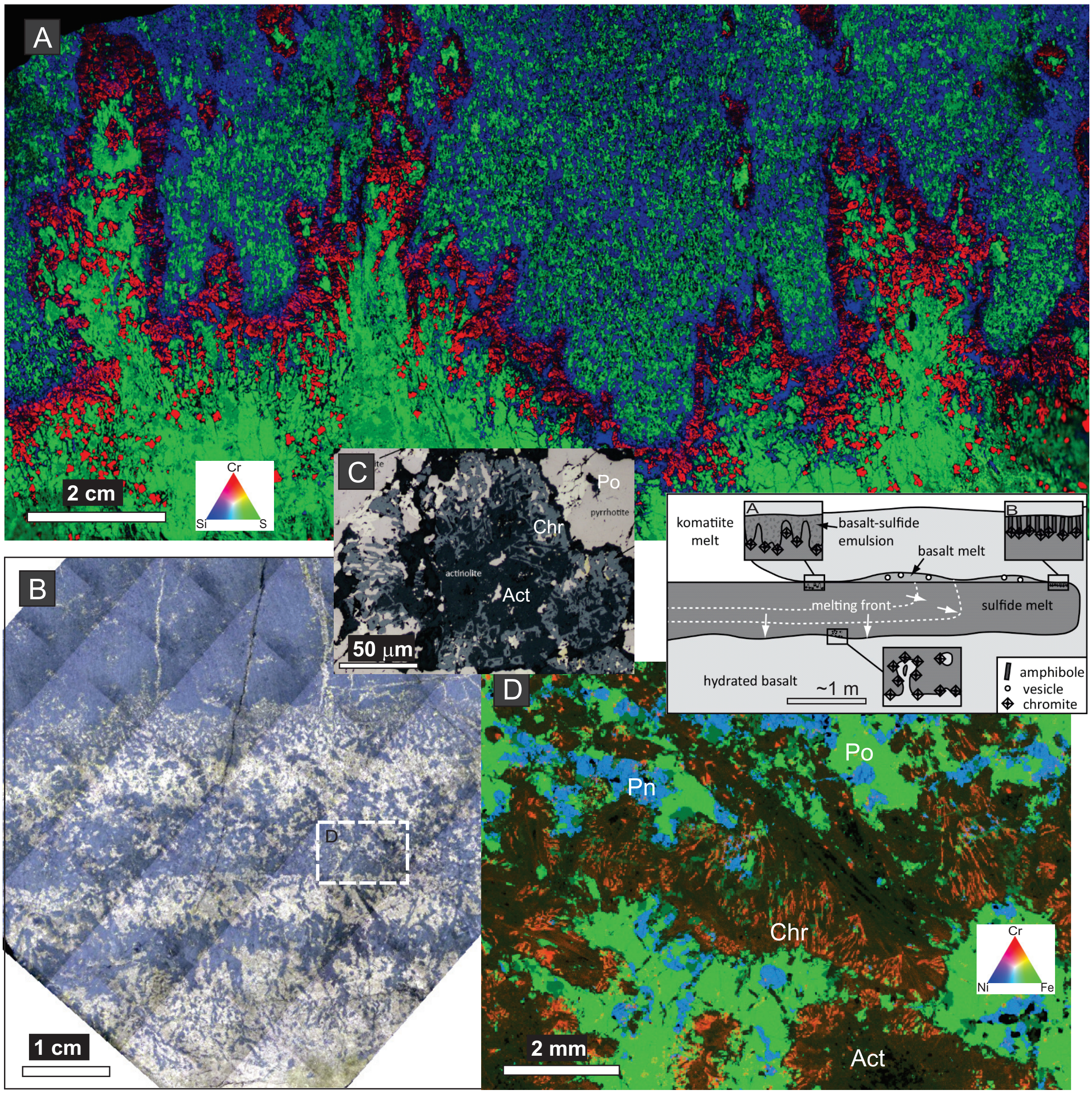
A
2 cm
Cr
Si
S
B
D
1 cm
C
Po
pyrrhotite
Chr
actinolite
Act
50 μm
komatiite
melt
A
basalt-sulfide
emulsion
basalt melt
B
melting front
sulfide melt
hydrated basalt
~1 m
amphibole
vesicle
chromite
D
Po
Pn
Chr
Cr
Ni
Fe
2 mm
Act

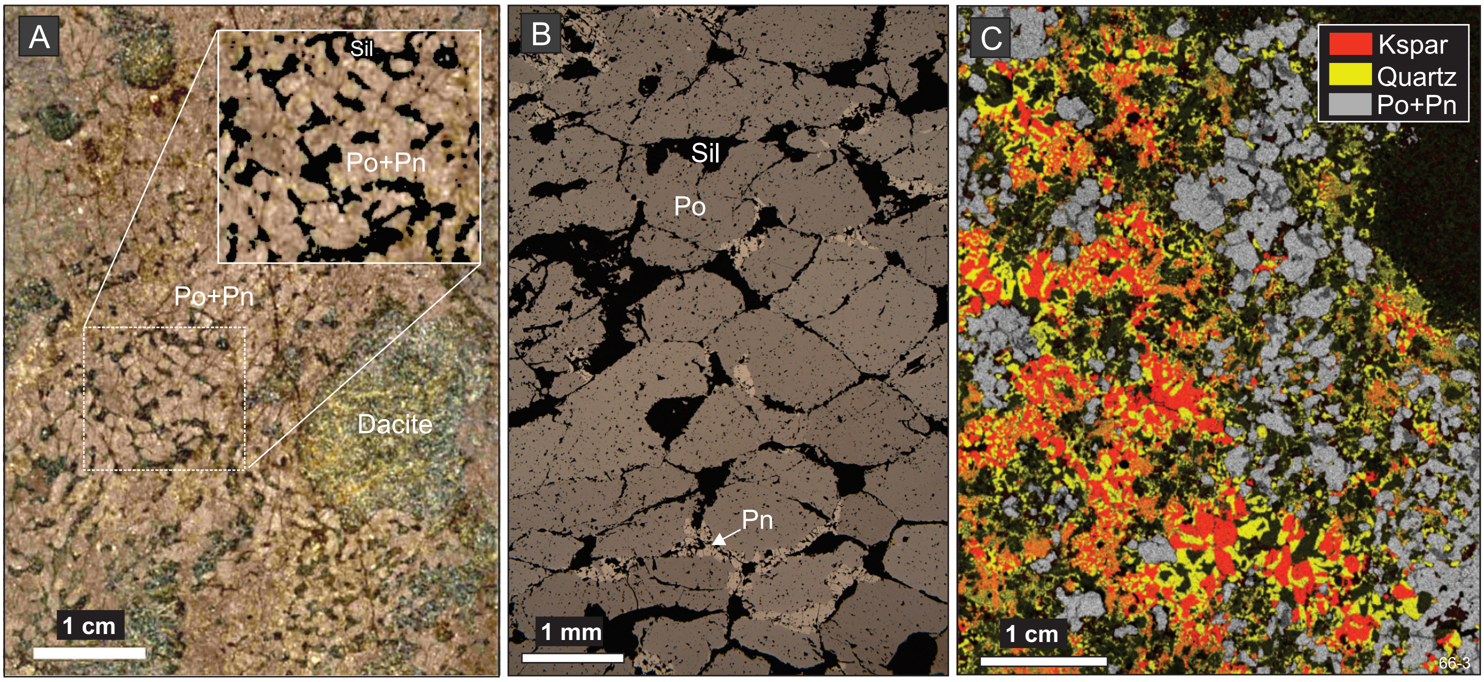
A
Sil
Po+Pn
Po+Pn
Dacite
1 cm
B
Sil
Po
Pn
1 mm
C
Kspar
Quartz
Po+Pn
1 cm
66-3

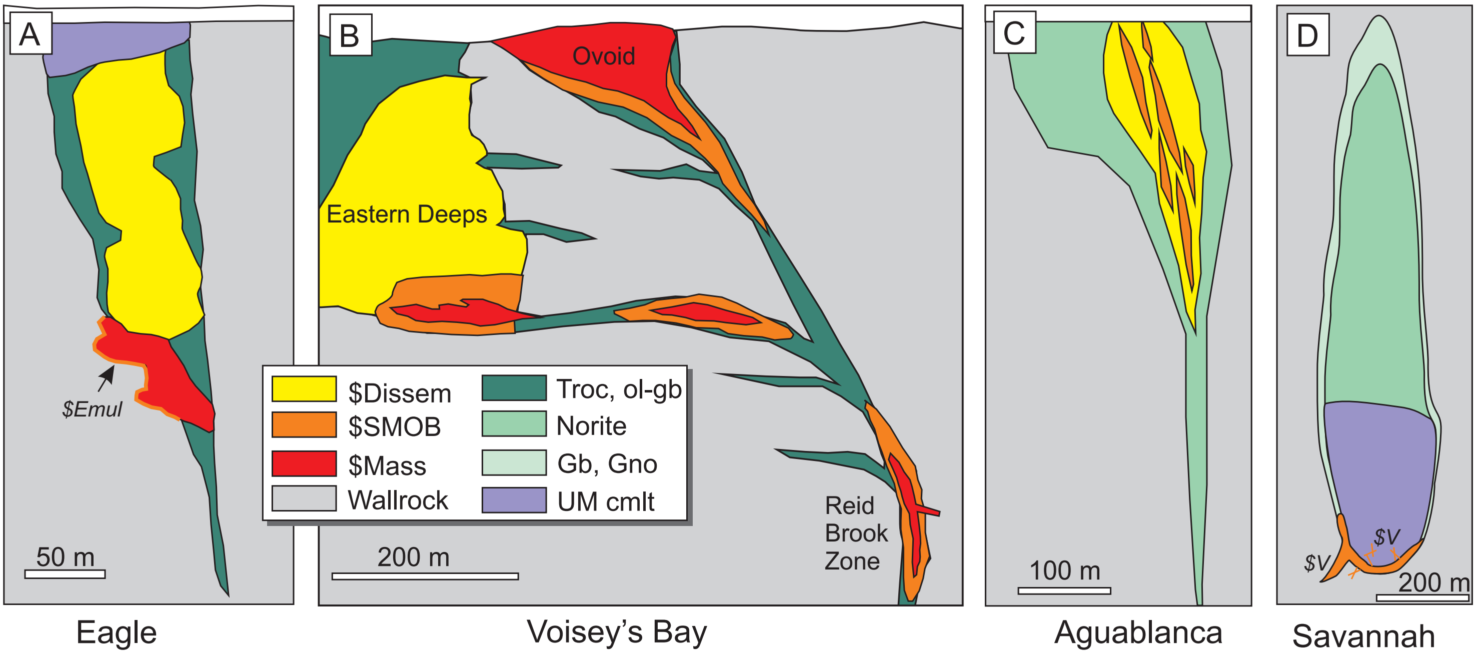
A
$Emul
50 m
Eagle
B
Ovoid
Eastern Deeps
$Dissem
$SMOB
$Mass
Wallrock
Troc, ol-gb
Norite
Gb, Gno
UM cmlt
Reid Brook Zone
200 m
Voisey's Bay
C
100 m
Aguablanca
D
$V
$V
200 m
Savannah

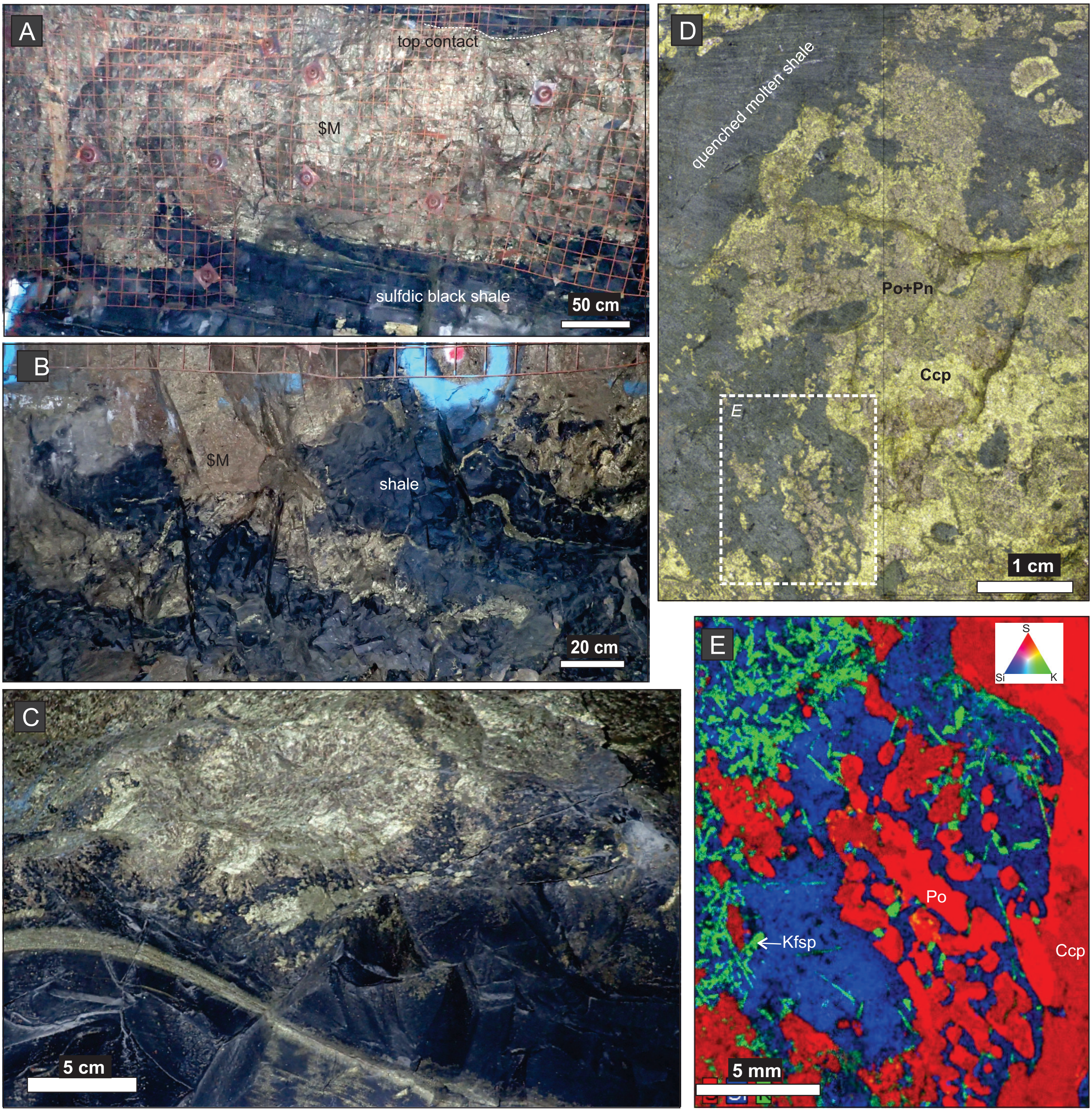
A
top contact
$M
sulfdic black shale
50 cm
B
$M
shale
20 cm
C
5 cm
D
quenched molten shale
Po+Pn
Ccp
E
1 cm
E
S
Si
K
Po
Kfsp
Ccp
5 mm

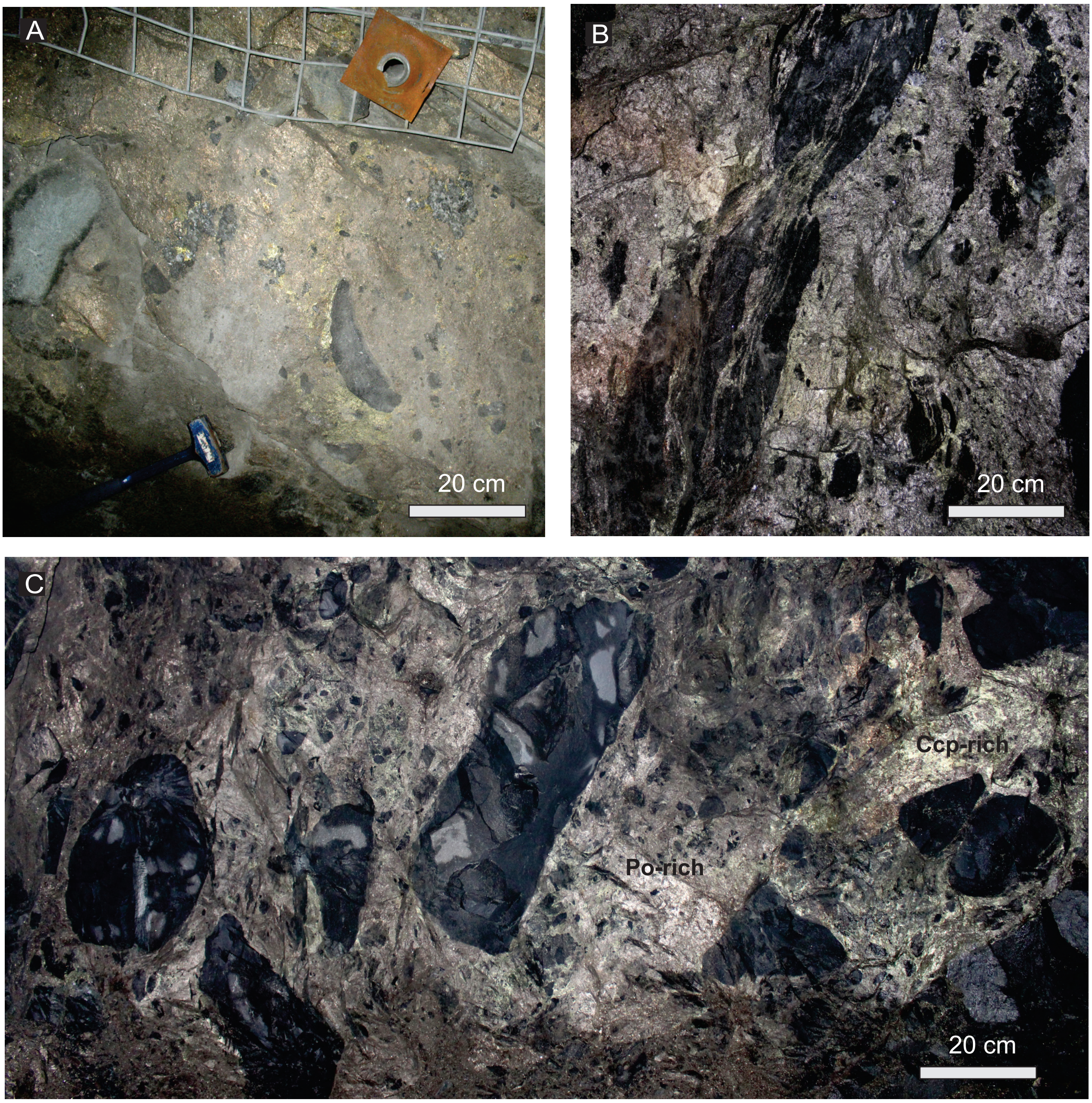
A
20 cm
B
20 cm
C
Ccp-rich
Po-rich
20 cm

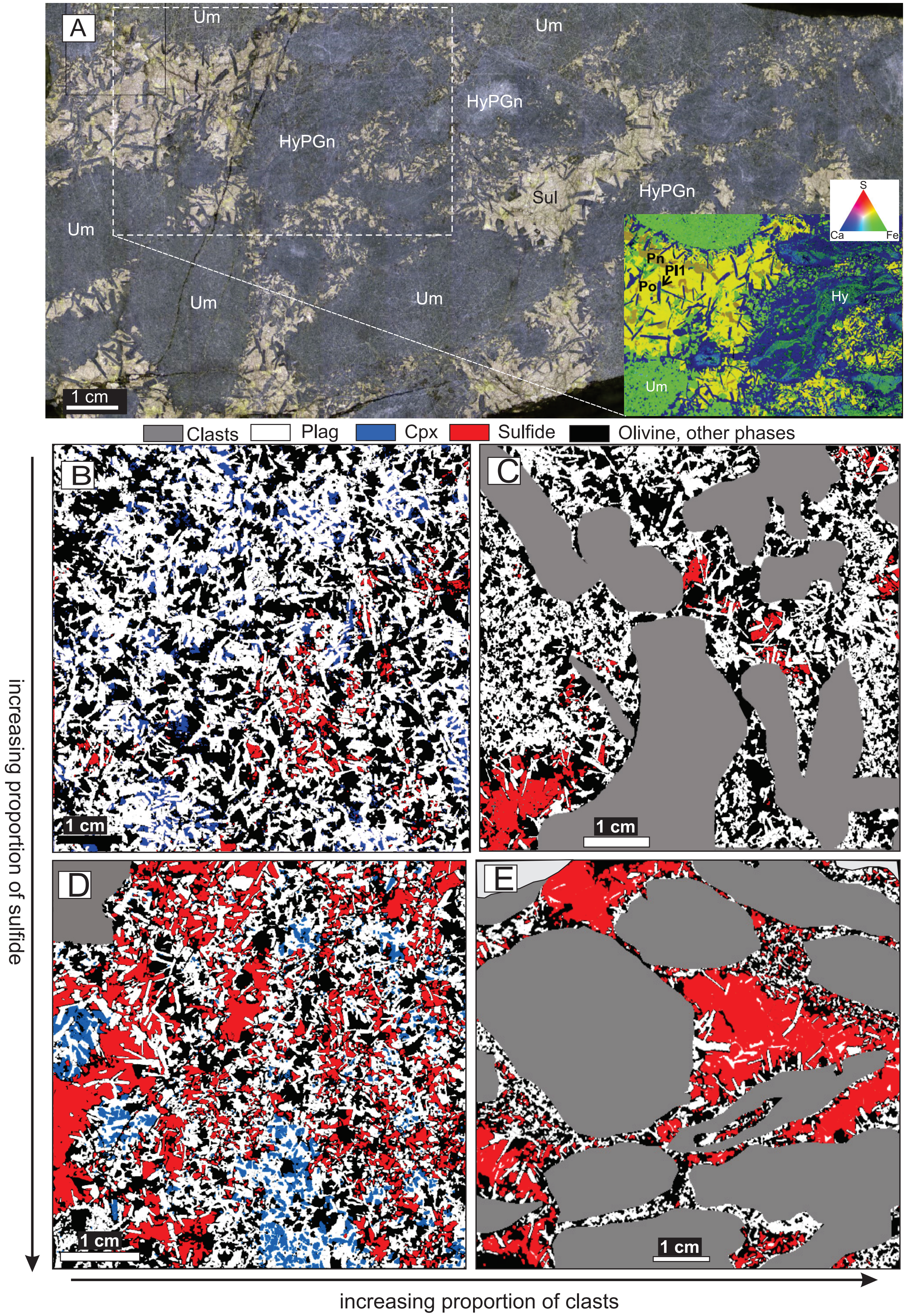

A
Um
Um
HyPGn
HyPGn
Sul
HyPGn
Um
Um
Um
S
Ca
Fe
Pn
Pl1
Po
Hy
Um
1 cm
Clasts
Plag
Cpx
Sulfide
Olivine, other phases
B
C
D
E
1 cm
increasing proportion of sulfide
increasing proportion of clasts

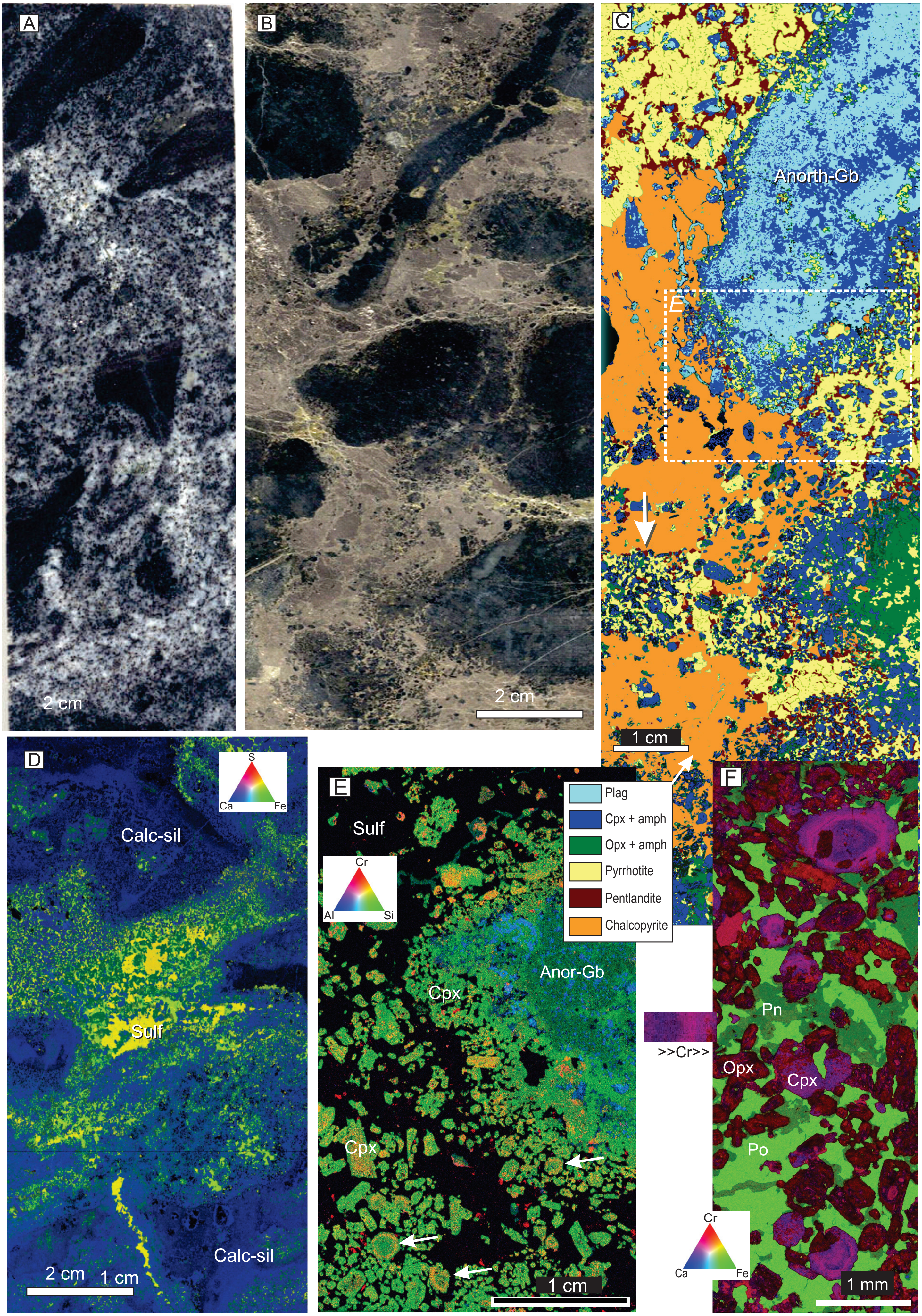
A
2 cm
B
2 cm
C
Anorth-Gb
E
1 cm
D
S
Ca
Fe
Calc-sil
Sulf
Calc-sil
2 cm
1 cm
E
Sulf
Cr
Al
Si
Cpx
Anor-Gb
Cpx
1 cm
Plag
Cpx + amph
Opx + amph
Pyrrhotite
Pentlandite
Chalcopyrite
>>Cr>>
F
Pn
Opx
Cpx
Po
Cr
Ca
Fe
1 mm

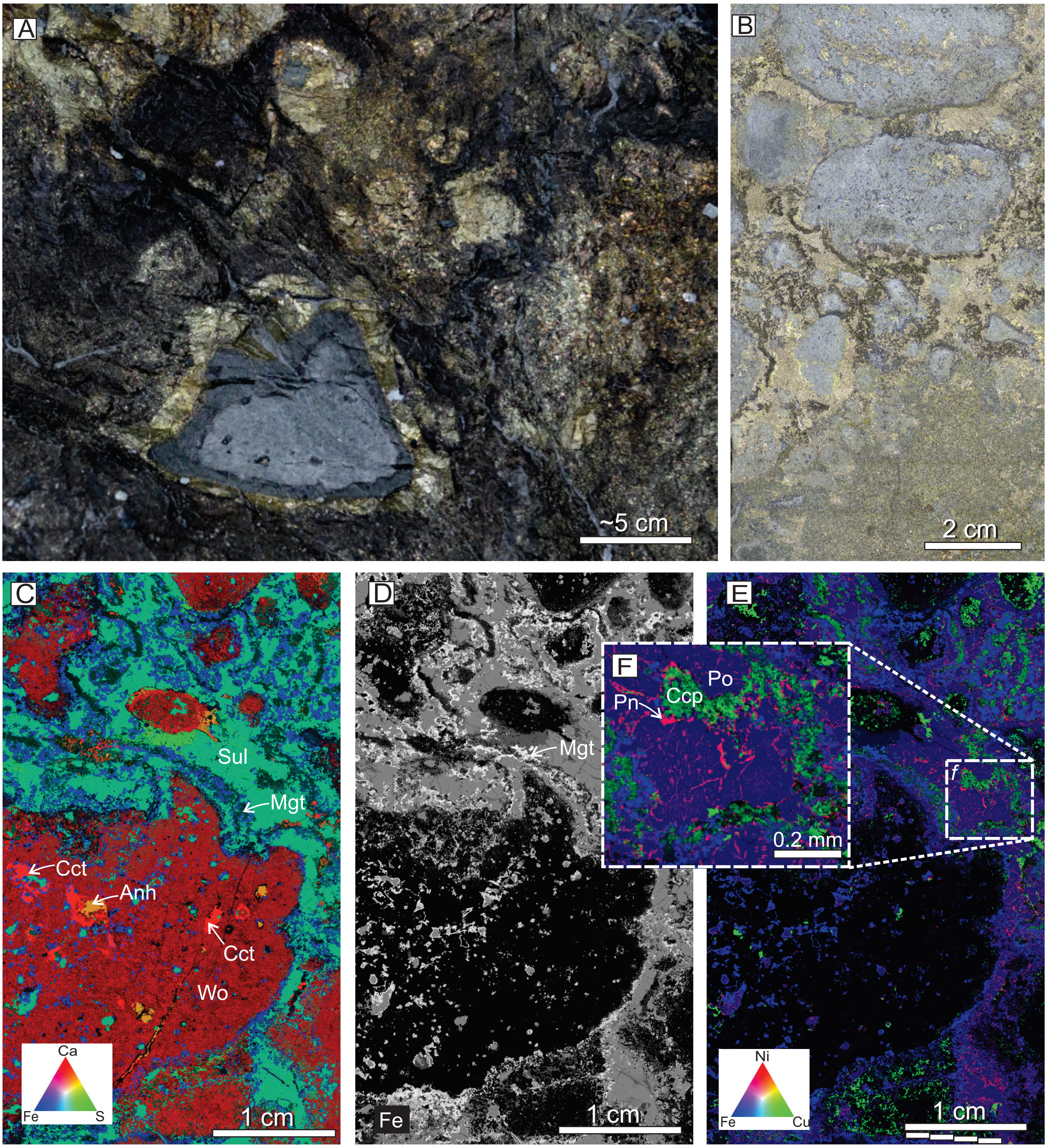

A
~5 cm
B
2 cm
C
Sul
Mgt
Cct
Anh
Cct
Wo
Ca
Fe
S
1 cm
D
Mgt
Fe
1 cm
E
F
Po
Pn
Ccp
0.2 mm
f
Ni
Fe
Cu
1 cm

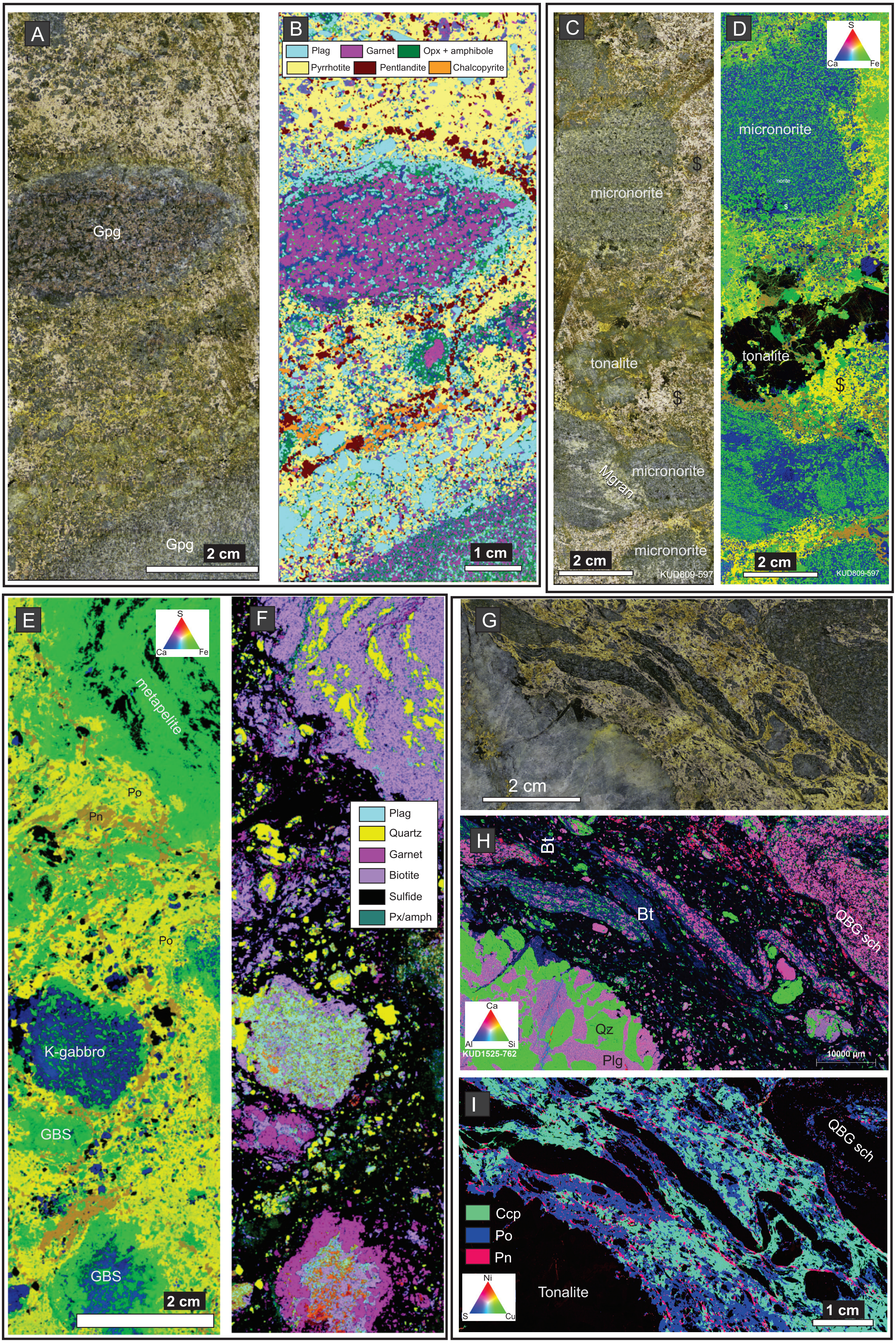
A
Gpg
Gpg
2 cm
B
Plag
Garnet
Opx + amphibole
Pyrrhotite
Pentlandite
Chalcopyrite
1 cm
C
micronorite
tonalite
Mgran
micronorite
micronorite
2 cm
KUD809-597
D
S
Ca
Fe
micronorite
tonalite
2 cm
KUD809-597
E
S
Ca
Fe
metapelite
Po
Pn
Po
K-gabbro
GBS
GBS
2 cm
F
Plag
Quartz
Garnet
Biotite
Sulfide
Px/amph
G
2 cm
H
Bt
Bt
QBG sch
Ca
Al
Si
KUD1525-762
Qz
Plg
10000 µm
I
QBG sch
Ccp
Po
Pn
Ni
S
Cu
Tonalite
1 cm

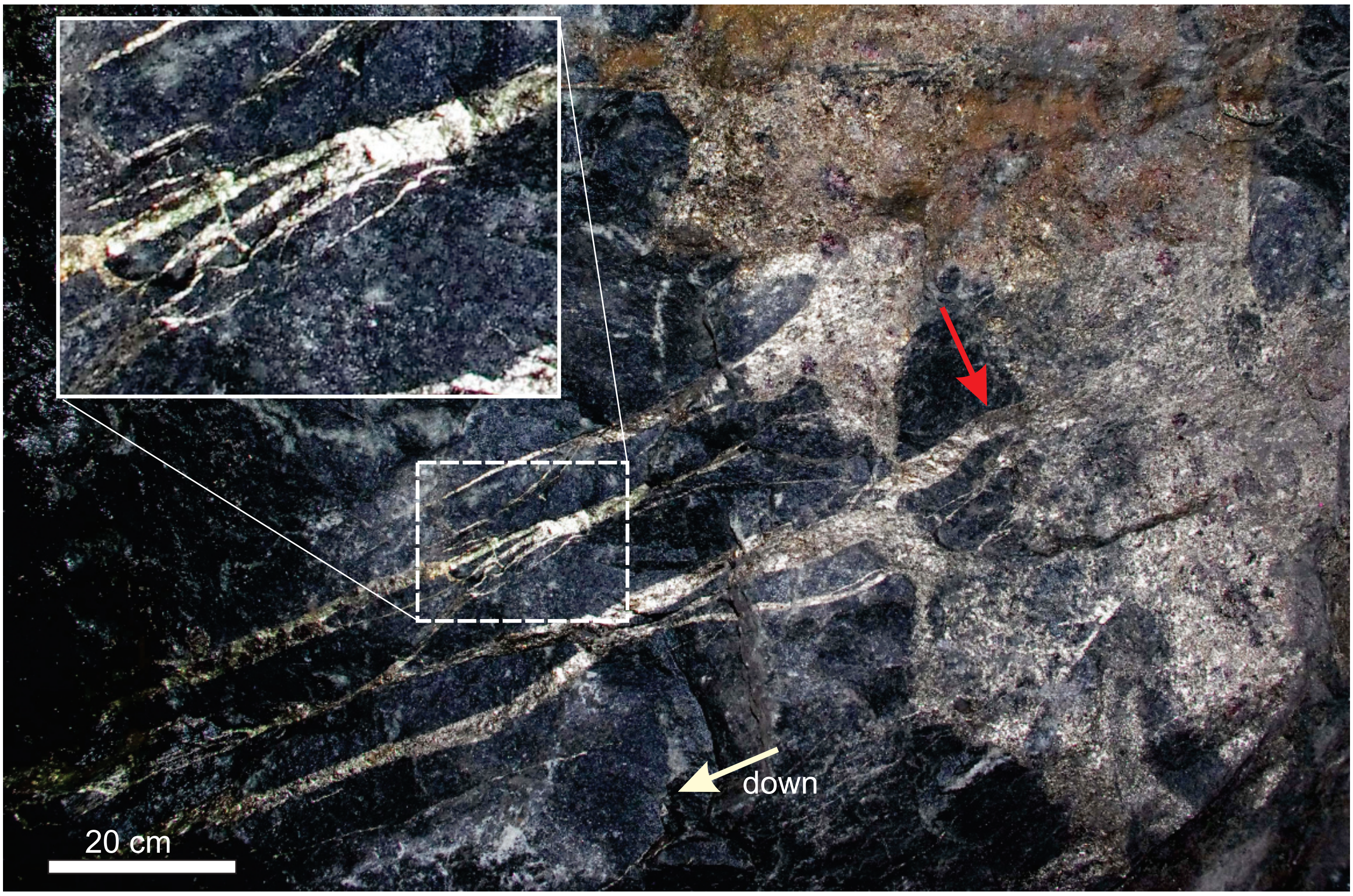

down
20 cm

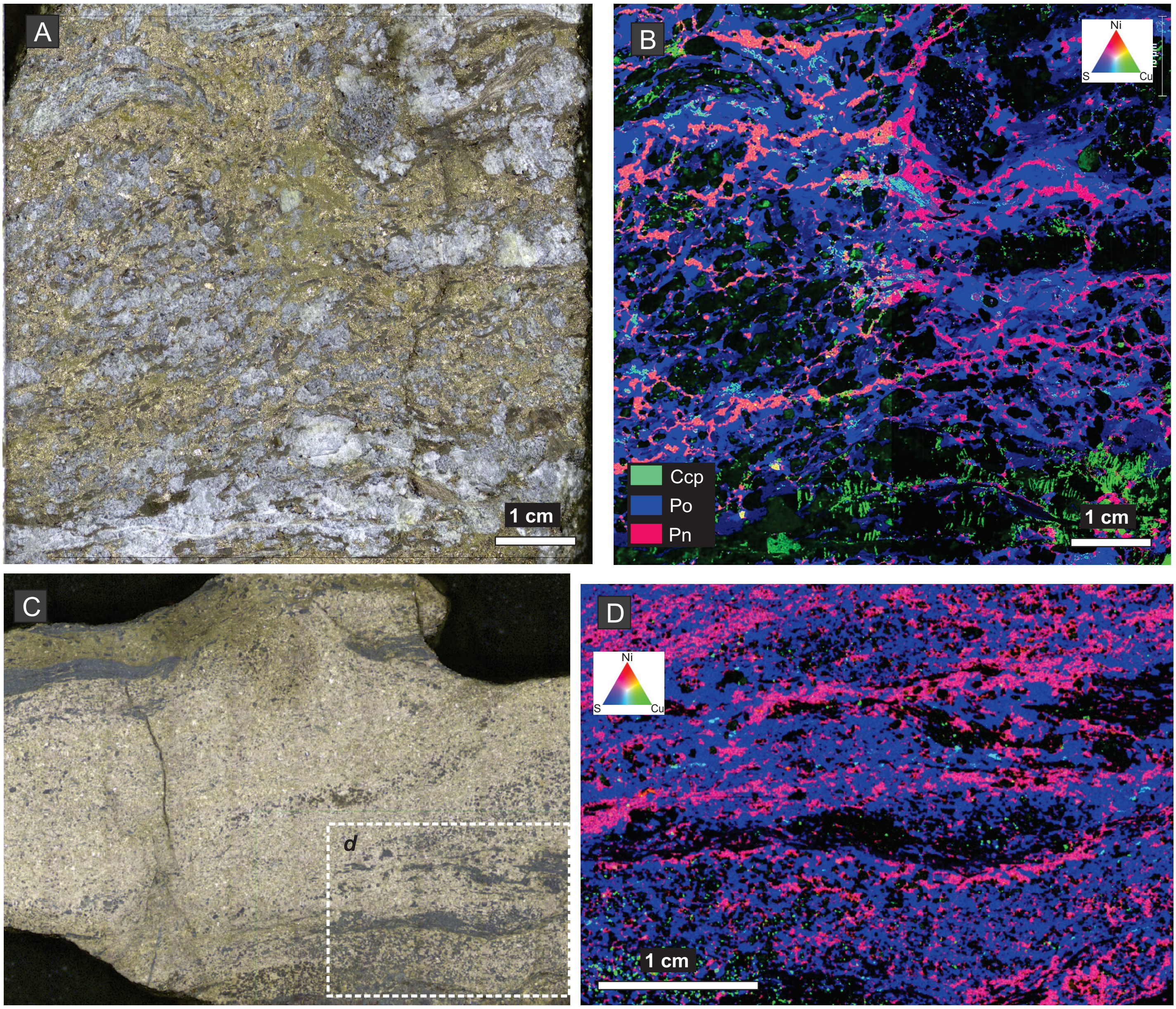
A
1 cm
B
Ni
S
Cu
Ccp
Po
Pn
1 cm
C
d
D
Ni
S
Cu
1 cm

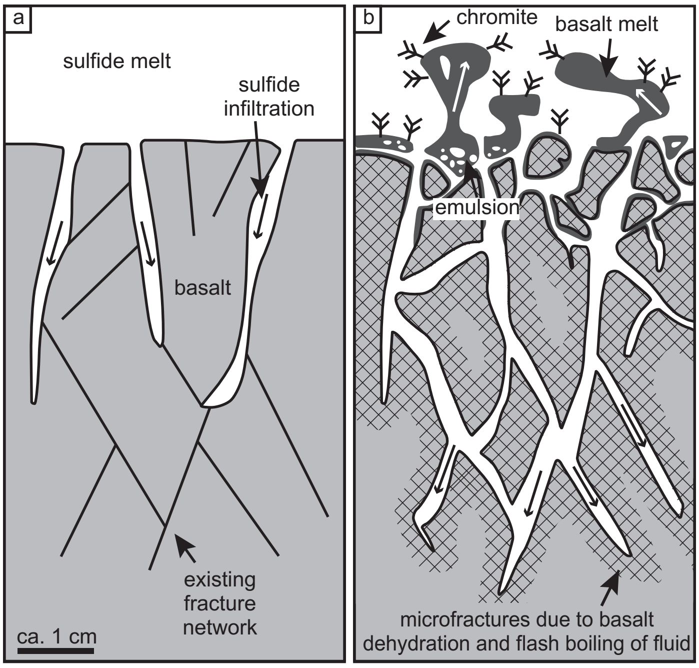
a
sulfide melt
sulfide
infiltration
basalt
existing
fracture
network
ca. 1 cm
b
chromite
basalt melt
emulsion
microfractures due to basalt
dehydration and flash boiling of fluid

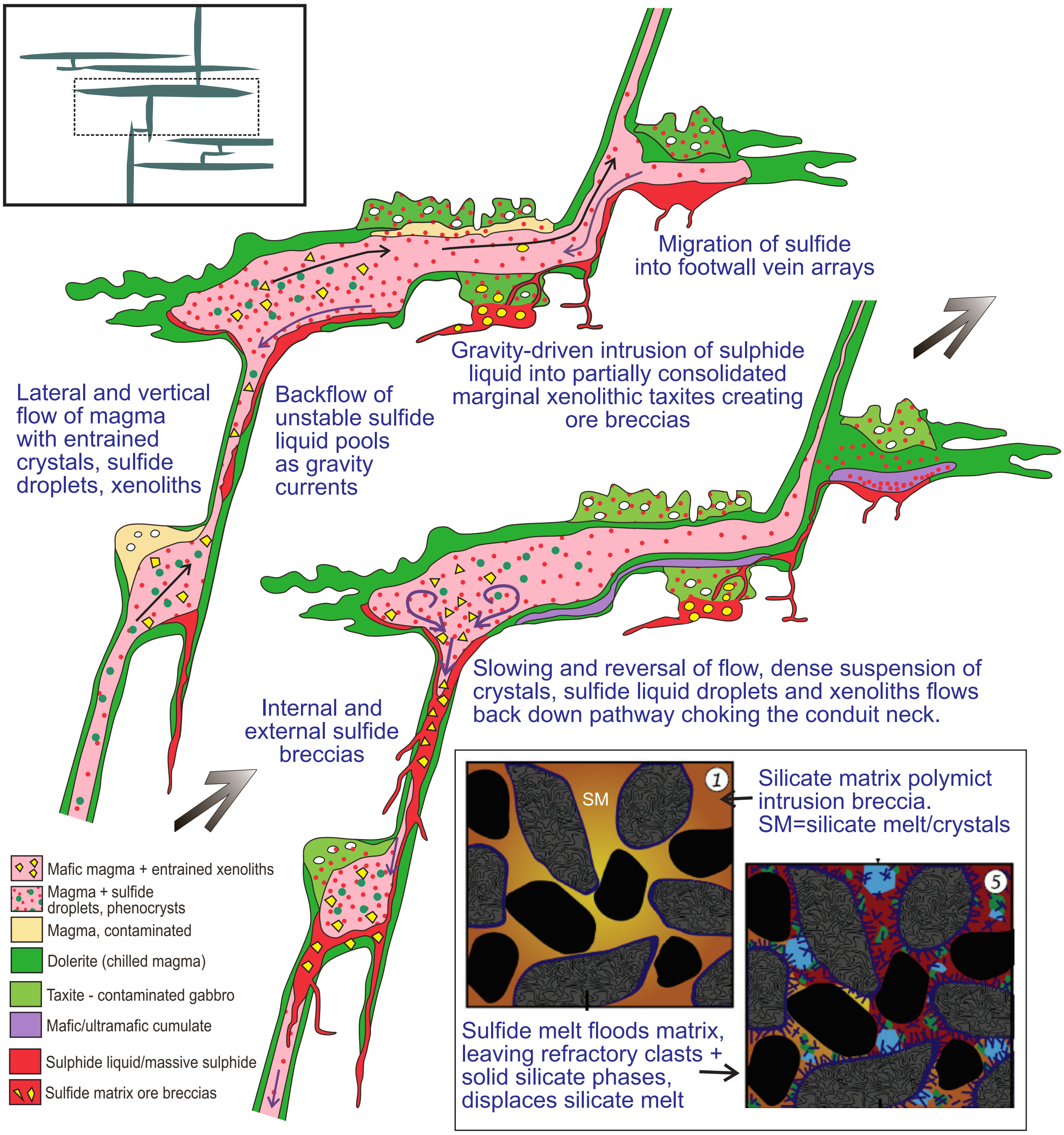

Migration of sulfide
into footwall vein arrays
Gravity-driven intrusion of sulphide
liquid into partially consolidated
marginal xenolithic taxites creating
ore breccias
Lateral and vertical
flow of magma
with entrained
crystals, sulfide
droplets, xenoliths
Backflow of
unstable sulfide
liquid pools
as gravity
currents
Slowing and reversal of flow, dense suspension of
crystals, sulfide liquid droplets and xenoliths flows
back down pathway choking the conduit neck.
Internal and
external sulfide
breccias
Silicate matrix polymict
intrusion breccia.
SM=silicate melt/crystals
SM
1
5
Sulfide melt floods matrix,
leaving refractory clasts +
solid silicate phases,
displaces silicate melt
Mafic magma + entrained xenoliths
Magma + sulfide
droplets, phenocrysts
Magma, contaminated
Dolerite (chilled magma)
Taxite - contaminated gabbro
Mafic/ultramafic cumulate
Sulphide liquid/massive sulphide
Sulfide matrix ore breccias

Table 1: summary descriptions of the main localities for samples illustrated in this paper

Deposit	Type, age	Characteristics of sulfide-rich ores	References
Moran, McLeay (W. Australia Yilgarn)	Komatiite hosted type 1*, Archean	Typical Kambalda style deposit, sulfides in linear embayment at the base of an entrenched lava channel, basaltic footwall	(Staude et al., 2016; Staude et al., 2017a; Staude et al., 2017b)
Silver Swan (W. Australia Yilgarn)	Komatiite hosted type 1*, Archean	Sulfides forming linear "shoot" at the base of an entrenched lava channel, dacitic footwall	(Dowling et al., 2004) (Barnes et al., 2017)
Eagle (Mid Continent Rift, Michigan, USA)	Conduit-style mafic-ultramafic intrusion hosted, Proterozoic	Large scale (tens of metres) injection of massive sulfides into wall rock shales, melt films and emulsion textured ores developed at contacts.	Ripley and Li (2011), Ding et al. (2012 a,b).
Voisey's Bay (Nain Plutonic Complex, Labrador)	Conduit-style mafic-intrusion hosted, Proterozoic	Pure massive sulfides (Ovoid) underlain by thicknesses of sulfide matrix ore breccias with distinctive plagioclase frameworks in the matrix; similar breccias also found at sill-dyke transitions and dyke bridges.	Ripley and Li (2011), Lightfoot et al., (2012), Barnes et al. (2017c); Evans-Lamswood et al., 2000.
Savannah (Halls Creek Orogen, W. Australia)	Sulfides in keel of blade-shaped dyke, Proterozoic	Predominantly polymict sulfide matrix breccias with abundant vein-hosted sulfide, transitional to tectonic durchbewegung breccias.	Hicks et al. (2017); Hoatson and Blake (2000).
Aguablanca (Variscan Orogeny, Spain)	Sulfides in core of funnel-shaped stock, Phanerozoic	Sulfide matrix breccias with halo of sulfide poor breccias and inclusion bearing, disseminated sulfide bearing gabbros.	(Casquet et al., 2001; Ortega et al., 2004; Tornos et al., 2006; Pina et al., 2010)
Oktyabrysky (Noril'sk-Talnakh camp, Siberia)	Mafic chonolith-hosted massive sulfides, super-giant deposit; Phanerozoic	Wide variety of ore types including globular, disseminated, massive, vein hosted; sulfide matrix breccias and skarn breccias at flanks of massive ores and in hanging wall; melt infiltration fronts, melt films and emulsion ores at base.	Naldrett (2004); Likhachev (1994); Sluzhenikin et al., 2014
Thompson (Trans-Hudson orogeny, Manitoba, Canada)	Komatiite dunite hosted intrusion, type 5, Proterozoic	Intensely deformed durchbewegung breccias and sulfidic mylonites almost entirely mobilised into granulite facies country rock paragneisses	(Lightfoot et al., 2017)
Spotted Quoll (Forrestania Belt, W Australia)	Komatiite hosted, type 5., Archean.	Sulfide-rich mylonites in off-contact shear zone, amphibolite facies, polydeformed.	(Prichard et al., 2013)
Frood, Sudbury (Ontario, Canada)	Impact melt sheet, Proterozoic	Wide variety of sulfide styles including clean massive and sulfide matrix ore breccias in contact settings and offset dykes, globular and disseminated interstitial ores, emulsion textured ores at base of contact massive ore bodies.	Lightfoot (2016), Hawley (1962)

Textural type and sub-varieties	Sub type	Distinguishing criteria	Examples
Sulfide matrix ore breccias (SMOB)		Presence of silicate clasts typically mm to cm in size, in a continuous matrix of magmatic sulfide commonly containing disaggregated or single crystals or interconnected crystal frameworks derived from the clasts, and/or from a now-displaced silicate matrix component. Little or no penetrative fabric within sulfides or at clast margins. Clasts are commonly concentrically zoned with respect to mineralogy.	
SMOB	SMOB – soft clast type, polymict	Margins of most clasts disaggregating into single crystals within sulfide, typical for clasts of non-refractory rock types, little or no fracturing of clasts.	Aguablanca, Savannah, Nebo-Babel
SMOB	SMOB-sharp-wall clast type, polymict	Margins of most clasts typically sharp but corresponding to original crystal boundaries, typical of clasts of refractory lithologies (dolerite, norite, carbonate, calc-silicate, anorthosite, "restite"). Note that some breccias contain both sharp-wall and soft clast types.	Voisey's Bay, Oktyabrysky skarn clast example.
Vein-array pseudobreccias		Monomict pseudo-breccias formed by shattering or extensive fracturing of initially homogeneous rock with sulfides invading the anastomosing fracture set. Typically "sharp-wall clast" although may show a transition upward through a melt-infiltration interface into emulsion textured ore.	Moran (Kambalda), Savannah, potions of Sudbury offset dykes.
Emulsion textures		Mixtures of sulfide melt and locally derived molten silicate showing highly sinuous and sometimes fractal contacts, formed either by physical stirring of two coexisting melts or by arrested detachment and ascent of silicate melt plumes formed initially in melt film layers along sulfide-silicate contacts. Silicate component may show quenching or rapid crystal growth features. May be closely associated with underlying vein-array breccias.	Moran, Eagle, Noril'sk, Aguablanca
Emulsion textures	"Inverted net-texture"	(Rare). Silicate phases interstitial to pyrrhotite crystals, reflecting final solidification of low-melting silicate component below the crystallisation temperature of original MSS.	Moran, Silver Swan, Nebo-Babel.
Tectonic (durchbewegung) breccias		Typically foliated (silicates and sulfides) with extensive disaggregation of silicate inclusions showing grain fracturing; microscale shear bands developed at silicate-sulfide contacts, folded clasts with axial planar fabrics, occasional development of C-S fabrics; deformation microfabrics recorded by	Savannah, Thompson, Spotted Quoll, Sudbury, Nebo-Babel

		pentlandite (implying sub-magmatic temperatures), locally mylonitic fabrics. (See Table 3).	
Tectonised magmatic breccias		Any type of breccia showing essential magmatic characteristics as defined above, but showing evidence of shearing and foliation development; may show complete transition to durchbewegung type.	Savannah

Table 2. Classification scheme for semi-massive and sulfide matrix ore breccias. For a full classification of magmatic sulfide ore textures, including disseminated and net textured ores, with illustrations, see electronic supplementary material.

Criterion	Magmatic sulfide-matrix breccia	Tectonic (durchbewegung) sulfide matrix breccia
Derivation of clasts	Monomict or polymict: country rocks and endogenous host intrusion	Monomict or polymict; where monomict, dominated by clasts of immediate wall rock.
Location	Various, usually at contacts between host magmatic body and country rock, sill-dyke transitions or intrusion necks.	Within shear zones localised by presence of sulfide layers.
Clast or matrix supported	Typically clast supported, although this may require 3D imaging to recognise, as clasts may form open 3D frameworks.	Either clast or matrix supported.
Clast contact relations	Depending on nature of clast – refractory clast types (e.g. carbonates) have sharp walls, non-refractory clasts such as pelitic metsediments or granitoids show marginal disaggregation along grain boundaries into crystal “clouds”, or development of “swirled” emulsion textures. May preserve delicate crystal frameworks inherited from original silicate matrix (e.g. Voisey’s Bay, Fig. 9). Molten clasts in emulsion textured types may show mineralogical reaction rinds between silicate and sulfide components, e.g. chromite-rich rinds at Kambalda (Fig. 4).	Typically sharp or marked by strongly localised shear bands along contacts and local reduction of grain size into mylonite bands. Clasts commonly folded. Clasts and sulfide matrix share common foliation and/or lineation (e.g. Spotted Quoll, Fig. 15). Where polymict, no correspondence between clast mineralogy and mineralogy of enclosing crystal “clouds” (e.g. Savannah, Fig. 13F). May develop C-S shear fabrics (shear bands oblique to foliation planes).